

Fish microfossils from Ramsåsa, site E, Scania, southern Sweden (mid Palaeozoic)

J.M.J. Vergoossen

Vergoossen, J.M.J. Fish microfossils from Ramsåsa, site E, Scania, southern Sweden (mid Palaeozoic). *Scripta Geologica*, **127**: 1-70, 9 pls., 3 text-figs., 17 tables, Leiden, May 2004.

J.M.J. Vergoossen, Grevingaheerd 261, NL 9737 SN Groningen, The Netherlands (e-mail: jmj.vergoossen@home.nl).

Key words — osteostracans, anaspids, thelodonts, acanthodians, Whitcliffian, Sweden.

Material from three pieces of rock from Ramsåsa, site E, was divided into size fractions 0.106, 0.212, 0.355, 0.425 and 0.5 mm. Larger sizes were absent. The three assemblages were examined and compared with each other, also per fraction, and with residue samples from site E. The latter are proportionately not representative of the faunas of which they must have been part, specimens measuring 0.5 mm or more. The residue labels refer to Ørvig and his student Peyel. The results of the comparison between the assemblages from the rocks and from the residues are hardly complementary. Thelodont scales were obtained almost exclusively from the pieces of rock; acanthodian 'modified trunk' scales, spines and jawbones and rare birkeniid remains were restricted to the stored residues, which also yielded a variety of osteostracan ('hemicyclaspid' and 'zenaspid') armour fragments. A late Ludlow age (within the *T. sculptilis* biozone) is suggested for the rock samples on the basis of the fish assemblages alone. Since the Ørvig and Peyel residue materials contained *T. sculptilis* scales, they are not older than the *T. sculptilis* zone (Upper Ludlow- Lower Pridoli).

Contents

Introduction	1
Material, registration, methods and preservation	2
Systematic palaeontology	3
Osteostracan fishes	3
Anaspid fishes; birkeniids	10
Thelodont fishes	11
Acanthodian fishes	22
Scale frequencies	40
Correlation	46
Acknowledgements	47
References	47
Appendix	51

Introduction

Four microvertebrate assemblages from Ramsåsa site E *sensu* Grönwall, 1897 (site 7 *sensu* Larsson, 1979, p.180), in Scania, southern Sweden are described and compared for the first time (Vergoossen, 2002c, fig. 1). The assemblages derive from one registered (P 434a) and three unregistered pieces of rock housed in the fish collections of the Palaeozoology Department of the Swedish Museum of Natural History (NRS). Several unregistered fish macro- and micro-remains from Ramsåsa E and separately

stored in Ørvig's cabinet in the department were also included in this study.

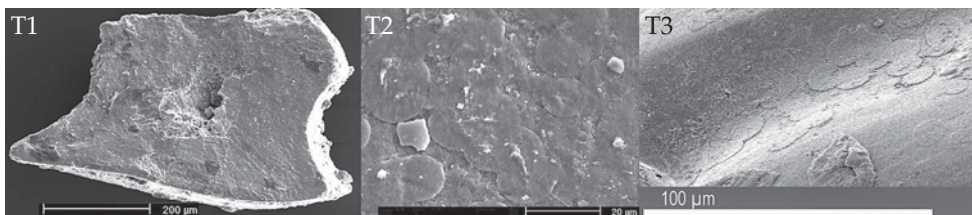
According to Larsson (1979, p. 180), site E was a small grindstone quarry already filled and covered with vegetation in 1879 and now destroyed. It was half way between Grönwall's Ramsåsa D, third exposure, and Ramsåsa F. The lithology consisted of reddish-brown silty mudstone and micaceous siltstone. The exposure yielded no tentaculites (Larsson, 1979; see also for further geographical references). Site E was in layer 4 *sensu* Grönwall (1897), now interpreted as the highest part of the Öved-Sandstone Formation (ÖSF) and dated as Pridoli by Jeppsson & Laufeld (1986). For age interpretations based solely on the microvertebrate faunas, see Vergoossen (2003a) and the correlation section below.

'*Nostolepis striata*' jaw bones (conventional identification), stored together with many acanthodian spines and shoulder girdle elements from site E samples, were excellently prepared by Ørvig's doctoral student Carl Peyel, who left the NRS as a result of a conflict about this material. Attempts to trace Peyel with the help of Ulf Borgen when the writer visited the NRS failed. Most of his material is not published. My chief aim was to provide a palaeontological, microvertebrate framework for site E in relation to the other Ramsåsa and Scania 'layer 4' localities, and for the further study of the Peyel acanthodian macro-remains.

For abbreviations, symbols and codes used in Tables 1-16, Plates 1-9 and Text-figures 1-3, see below and the caption to Table 1. Otherwise, abbreviations, symbols and glossary as in Vergoossen (2003a).

Material, registration, methods and preservation

The small, unregistered pieces of sampled rock available for examination were given serial working numbers SW 14, 15, 32. They weighed *c.* 17, 11 and 61 g, respectively. SW 14 has a label reading "diverse placoid scales" and also contained invertebrates, mainly gastropod and few phosphatized tentaculitid moulds. The partly hand-written label with SW 15 said "diverse placoid scales, *Thelodus* spp, collected and identified by Stensiö." The residue contained tentaculitids, fragments of brachiopods or bivalves, and one ostracode. Sample SW 32 had a label with "E. Stensiö 1924" on it, and yielded moulds of gastropods, tentaculitids and ostracodes. These three pieces of Ramsåsa E rock might have come from a different level or levels than the samples used by Larsson (see above, but cf. 1979, p. 18). Some of the fish scales from SW 32 are covered with thin, discoid, smooth, inorganic, probably calcium phosphate structures, *circa* 12-20 µm in diameter



Text-fig. 1. Vertical section of *Thelodus parvidens* scale, Ramsåsa E (sample SW 32), P9217.

Text-fig. 2. Detail of surface (of the neck) in Text-fig. 1, with discoid structures.

Text-fig. 3. Discoid structures on *Thelodus sculptilis* crown, Ramsåsa C (Vergoossen, 2003b, fig. 50).

(Text-figs. 1-3; Fig. 32, also Figs. 36, 44, 52, but not well visible without higher magnifications). The phenomenon has not been reported from invertebrates of the Öved Ramsåsa Group and Jeppsson (pers. comm.) has never seen anything like it on the conodonts (see also Vergoossen, 2003a, chapter 6). P434a contained a hand written label reading "Onchus?" (determination by Lehman). This sample was not dealt with in detail.

For dissolution procedures, see Vergoossen (2002c, 2003b). The residues were sieved into fractions with the mesh widths 0.106-0.212-0.355-0.425-0.5 mm. Fossils and sediment were not further separated by any other technical method.

One glass tube contained additional (selected) material from Ramsåsa E, especially fragments of acanthodian spines. On a printed sticker glued to the tube was written "Coll. Peyel" in Ørvig's handwriting. Few thelodont scales could be picked and identified from bits of sediment in the tube and adhering to bone. Six cardboard slides with few remains identified and selected/stored(?) by Ørvig were also studied. Ørvig's identifications (in pencil on the board) have been stated together with mine when they differ. It is not known whether the fossils in the glass tube or the slides were obtained from one or several samples or from one or several levels. Specimens from Helvetesgraven figured for their histology derive from the residue described in Vergoossen (1999b).

Systematic palaeontology

For general remarks, see Vergoossen (2002c). All measurements were taken on largest diameters, unless stated otherwise.

Osteostracan fishes (from the Peyel residue)

Osteostracan scales and armour fragments; body of fish not known Figs 1-10.

Remarks — 'Body of fish not known' means that, concerning these fragments, no information is available on the composition and topography of the external dermal cover in complete specimens and the taxon is indeterminable within the classificatory label presented (that is, osteostracan fishes). The aim is to map the diversity of the osteostracan remains and compare them with other Scanian (ÖSF) osteostracan microfossils. For the quantitative significance of the latter in the Ramsåsa E assemblages, see section on scale frequencies (Tables 1-3). No forms with a tubercular exoskeleton or with an exoskeleton of "Thelodus-like scales" (as described by Ritchie, 1967, p. 80, from the ventral visceral exoskeleton of *Ateleaspis*) were observed. Recognizable fragments of cornual processes or polygonal plates with their natural boundaries intact were also not observed (cf. Fredholm, 1990, fig. 8a).

Descriptions — The flat and thin (c. 0.3 mm, measured where the plate is most complete; Fig. 1c), polygonal, perforated fragment P9142 (Fig. 1) shows a narrow strip on one side (upper in Fig. 1a) where the top layer is not preserved. Fracture lines divide this external layer into three parts. The small round openings (of the vascular

Table 2. Jawless fishes from Ramsåsa E, sample SW14 (fully picked). Taxa $\geq 5\%$ in bold.

Fraction	0.106	0.212	0.355	0.425	0.5	Total	% AgT
Number of taxa: 14 (¹ not counted)	9	10	7	8	8		
osteostracan fishes					1	1	0.1
thelodont fishes							% TT
<i>Thelodus parvidens</i> s.s.*	25	111	31	53	91 [1 T]	311 [1 T]	45.3
head scales		1	4	4	3	12	1.7
forma <i>Thelodus pugniformis</i>		1				1	0.1
forma <i>Thelodus bicostatus</i>	1		1			2	0.3
forma <i>Thelodus trilobatus</i> multicuspid	13 [7B]	19 [2B]	2	4	2	40 [9B]	5.8
forma <i>Thelodus trilobatus</i> monocuspid	1	2				3	0.4
variant 1*		1				1	0.1
<i>Thelodus traquairi</i>	1	11	4	3	1	20	2.9
<i>Thelodus</i> sp. indet., forma <i>baltica</i>				1		1	0.1
<i>Thelodus sculptilis</i>	52	75		6	25	158	23
forma <i>Thelodus radius</i>	9	16	8	13	9	55	8
<i>Thelodus sculptilis</i> or <i>T. parvidens sensu</i> Märss, 1986 ⁽¹⁾	1	12	3	5	3	24	3.4
<i>Thelodus</i> sp. indet., forma <i>subulata</i>	20					20	2.9
<i>Thelodus</i> sp. indet., diverse forms	8	3	9	7	10	37	5.4
Total jawless fishes	131	252	62	96	145	686	
Total thelodont fishes	131	252	62	96	144	685	
% of 685	19.1	36.8	9.1	14	21		

large ridges extend twice as deeply below the surface as their external height ('iceberg effect'). The cross sectional view (Fig. 2c) indicates that the thin, sheet-like ridge walls can extend across the entire vertical diameter of the plate. The ridges are interconnected sheet- or wing-like; these interconnections are lateral extensions of the ridges. Both ridges and interconnections bear dense, fine, parallel and longitudinal stripes (ultra-sculpture). On the ridge sides the stripes are diagonal, meeting at the ridge top (open angle facing antieriad). The stripes are usually straight, but can also curve to the ridge top (Fig. 2d). In some places, probably one longitudinal row of openings is situated between two ridges; each opening is separated from the next by an interr ridge connection. One semicircular ridge (Fig. 2d) shows cross-striping at high magnification. Zenaspid? *sensu* Gross (1961) mode of growth.

P9041 (Fig. 3) shows four rows of irregular, smooth, flattened ridges on a slightly curved plate fragment. The ridges rise above the plate. Relicts of parallel diagonal stripes on the ridge walls are only faintly visible (Fig. 3a). The most anterior ridges (Fig. 3a) widen out posteriad. Two anterior ridges curve up from the surface layer. Several ridges are complex structures consisting of two or more longitudinally fused shorter ridges (lowermost row in Fig. 3b). Lateral extensions also occur. Many external openings (of the vascular system) were eroded and only the longitudinal separation between the openings remains.

The arched fragment P9050 (Fig. 4) might represent an older growth phase of the previous fragment, with interconnections between the irregularly sinuous, shorter and longer ridges that have smoothed and flat tops. Ridges and interconnecting, vertical

Table 3. Jawless fishes from Ramsåsa E, sample SW15 (selection). Taxa $\geq 5\%$ in bold.

Fraction	0.106	0.212	0.355	0.425	0.5	Total	%AgT
Number of taxa : 20 (¹ not counted)	11	18	11	12	13		
osteostracan fishes	1	5		1	1	8	0.5
hemicyclaspid		3	1	1		5	0.3
thelodont fishes							% TT
<i>Thelodus parvidens</i> s.s.*	65	117	124	116	165	587	39.1
forma <i>T. costatus</i> *		2		1	1	4	0.3
other head scales	4	2	4	3	6	19	1.3
forma <i>Thelodus querceus</i>		1		1		2	0.13
forma <i>Thelodus bicostatus</i>	2	8		1	4	15	1
forma <i>Thelodus trilobatus</i>							
multicuspid	22 [19B]	35 [27B]	8 [7B]	12 [7B]	2 B	79 [62B]	5.3
monocuspid	2	3			1	6	0.4
forma <i>Thelodus clavaeformis</i>							
Lehman, 1937		1				1	0.07
variant 1*		1	1			2	0.13
variant 2*					1	1	0.07
variant 3*					1	1	0.07
<i>Thelodus traquairi</i>	5	39	15	11	11	81	5.4
<i>Thelodus</i> sp. indet., forma <i>baltica</i>		2	1	1		4	0.3
<i>Thelodus sculptilis</i>	150	136	104	61	58 ²	509	33.9
forma <i>Thelodus radiosus</i>	19	19	33	23	23	117	7.8
<i>Thelodus sculptilis</i> or <i>T. parvidens</i> sensu Märss, 1986 ⁽¹⁾		10	10	6	5	31	2.1
<i>Thelodus</i> sp. indet., forma <i>subulata</i>	18	2				20	1.3
<i>Thelodus</i> sp. indet., diverse forms	1	10	8	3	1	23	1.5
<i>Paralogania ludloviensis</i>		1?				1?	0.07
Total jawless fishes	289	397	309	241	280	1516	
Total thelodont fishes	288	389	308	239	279	1503 = 91%	
% of 1503	19.2	25.9	20.5	15.9	18.6		

² This figure is too high, because it represents the number of scales picked from this fraction rather than the *size* of the scales.

walls enclose large pore? spaces. The smaller openings of the vascular system can be seen at the foot of the ridges (Fig. 4a, bottom left) and in cross-section (Fig. 4b, bottom right). The close-up (Fig. 4c) shows relicts of fine, diagonal parallel striping (ultra-sculpture) on the ridge walls and the connections between the ridges; it also shows the formation of new ridges where the interconnecting walls meet. Some of the longer ridges may be complex, longitudinally apposed structures. *Zenaspid?* *sensu* Gross (1961) mode of growth(?); compare with Vergoossen (2003b, fig. 5) (Ramsåsa C).

Several 'longitudinal', smoothed and flattened, curved and subparallel ridges are seen in P9051 (Fig. 5). These ridges begin more or less at the same level and are separated by two to three rows of apertures. The surface between the ridges is concave. The rightmost ridge is latitudinally connected at one end to (the beginning?) of the inserted and broken ridge. Compare Vergoossen (2003b, fig. 3) (Ramsåsa C).

Worn and damaged rectangular scale P9057 (Fig. 6) shows an unornamented,

lowered and slightly concave overlap area with parallel lamination. Just below the ridged external surface, a single row of fairly large openings of the vascular system is seen (Fig. 6a), more or less parallel to the orientation of the ridges, which presumably indicates the long axis of the trunk. The diameter of these openings varies from *c.* 64×57 (largest) to *c.* $46 \times 35 \mu\text{m}$ (smallest). The crown edge adjoining the overlap area has a narrow smooth zone (Fig. 6b). Beyond this follows a tuberculated zone. The small subrounded to ellipsoid tubercles are surrounded by a single row of smaller surface openings, less than $20 \mu\text{m}$ in diameter. In continuation of the tubercles, rows of elongate low ridges are situated. These can be interconnected. Orientation of tubercles and ridges are diagonal and posteriad. In lateral view (Fig. 6b), the large cavities of the middle layer can be observed. *Zenaspid?* *sensu* Gross (1961) mode of growth?

P9058 (Fig. 7) shows the cross laminated bone of the basal layer and the relicts of its vascularisation, elongate wide and concave spaces for vessels. To the left are the overlying, much smaller and rounded openings such as occur at the foot of the external ridges.

In P9059 the sculptured layer with the ridges is divided into halves; where these meet there is a double row of thin and low, smooth triangular or rounded bladelets facing each other (Fig. 8). A boundary line and groove separate one row of blades from the other. This demarcation is situated at the top of a plate like a low gable roof. The dentine ridges on both halves are probably oriented posteriad and longitudinally, which is at a right angle to the dividing groove. On the internal side, the plate is concave posteriad (in the direction of ridge orientation; Fig. 8c). The slope of the plate is steeper on the left (Fig. 8c) than on the right, and one or two ridges on the steep slope lean leftward. Each ridge forms the top of a round, perforated 'mount' with convex, rather steep, anterolateral slopes. The perforations represent vascular openings of the 'infundibular' type (see variant 2; Vergoossen, 2003b, fig. 6). Size of outer ring of openings measured varies between *c.* 22×19 and *c.* $41 \times 32 \mu\text{m}$. The outline of each mount is clearly indicated (Fig. 8c). The ridges slope up, tapering. Their dorsal surface is flat and smooth. Ultrasculpture was not observed. Where the ridges are broken, an interior hole (pulp cavity?) is visible. Ridges arranged in rows. The perforation of the sculpture-free and rather wide marginal area (Fig. 8a) is not as dense as on the mounts, and the openings are larger; this probably represents the middle layer (also seen in the gable).

P9062 (Fig. 9) is reminiscent of P9050 (Fig. 4), but pores are absent. In some places connecting walls have formed between the short, lumpy ridges. The surface perforations relate to the vascular system. Size of openings measured ranges from *c.* 8×8 to *c.* $18 \times 25 \mu\text{m}$. The ridges are 'mounted' on steep socles, which are not of the neat, uniform kind seen in the previous fragment. Tubercular structures (relicts of connecting walls?) can also be observed (Fig. 9a, upper part of photo). The fragment is more strongly curved (Fig. 9b) than P9050 (Fig. 4), the curvature is eccentric. *Zenaspid?* *sensu* Gross (1961) mode of growth?

P9106 (Fig. 10) is reminiscent of P9142 (Fig. 1), but differs in several aspects. No particular arrangement of the external openings can be observed. Low elevations occur on the perforated surface; one of these bears a low, smooth, sloping ridge. The shape of the openings is irregularly round. Measured diameter of openings varies between *c.* 15×14 and *c.* $28 \times 25 \mu\text{m}$. The walls around the openings might show

worn ultrasculpture of short, parallel straight stripes, oriented in the same direction as the ridge. A marginal, natural suture or boundary with a smooth sheet of bone still attached, would seem to be present on the edge anterior in the photo. Thickness of fragment *c.* 0.1 mm (elevations not considered). As in P 9142, the visceral side of the fragment is flat. *Hemicyclaspis*?

Morphology and taxonomy. Little is known about the morphological diversity of Scanian osteostracan microvertebrate remains from the ÖSF (or from the Klinta Formation). Lehman (1937, pp. 64, 75-77, 88) mentioned 'tremataspids' from Ramsåsa (site F), 'cephalaspids' from Ramsåsa (*idem*) and Öfvedskloster (= Övedskloster) and figured histological sections of both (pl. 6, figs. 6, 7; pl. 7, fig. 10). Vergoossen (1999b, 2002a, 2003b) identified (*cf.*) *Hemicyclaspis* from Helvetesgraven and Ramsåsa sites C, H. This taxon was considered a cephalaspid close to Early Silurian *Ateleaspis* from Scotland (e.g., Ritchie, 1967), but is now phylogenetically interpreted as a terminal taxon, as is *Ateleaspis* (Janvier, 1996). Janvier (*pers. comm.*) collected *Hemicyclaspis* from the same locality as that in the Burgsvik sandstone on Gotland from which Spjeldnaes (1950) erroneously reported *Cephalaspis*. Until details of the exoskeletal ornament of *Hemicyclaspis*, including the material from Gotland, are published, uncertainty about the generic identity of 'similar' Scanian microvertebrate remains and their place on the body, will continue to exist. Blicek & Janvier (1999, fig. 9.6) distinguished a *Hemicyclaspis* agnathan zone and a *Hemicyclaspis-Auchenaspis* (a primitive thyeostidian) community for the lower Pridoli of the Welsh Borderland in a brackish marine environment "represented by alternating calccretized mudstones and *Lingula*-bearing sandstone mudstone sequences." They further wrote (p. 85) that *Hemicyclaspis* always occurs "in strongly crossbedded sandstones." The Scanian rock samples with osteostracan microvertebrate remains have a considerable calcareous component and show no layering. For all these reasons, the Scanian osteostracans should be assigned to genus level (in this case, *Hemicyclaspis*) with caution. Nevertheless, the exoskeleton of *Hemicyclaspis* and its allies can provide useful information about what one might expect to find in the Scanian samples.

As regards the morphology of osteostracan microvertebrate remains from contemporaneous (Late Ludlow) Baltic remains, particularly from the standard sequence, the situation is a little better. Märss (1986, p. 90) noted the first appearance of *Zenaspis?* sp. in the Kuressaare Stage and the distribution of this species seems largely restricted to the late Whitcliffian Tahula Beds. Other osteostracan remains from these beds include Cephalaspidida and Cephalaspididae gen. et sp. indet. Trunk scales(?) of this latter, from the Tahula 709 core (-7.7-7.8m) were illustrated (*op. cit.*, pl. 25, figs. 8, 9), but these scales do not resemble any Scanian material. The morphology and histology of '*Zenaspis?*' sp. indet. was described and illustrated by Gross (1961) from erratics that are at least partly (Bey 36, 37) of Early Devonian age (*Turinia* faunas). Morphologically, there are certainly considerable similarities between some of the Scanian remains and '*Zenaspis?*' sp. indet. (e.g., perforated exoskeleton without distinct ridges, exoskeleton with ridges separated by perforated grooves, shape of ridges), although these features seem also present in *Hemicyclaspis*. Histological features of '*Zenaspis?*' sp. indet. (primary and secondary dentine ridges and covers, in several growth phases) have also been observed (Fig. 2; also below). Märss (1986) did not figure or discuss '*Zenaspis?*' sp. and

I assume that this name indicates likeness to the specimens figured by Gross (1961). Whatever may be the diagnostic value of the ornament on the *Zenaspis?* remains from erratics (cf. Blom, 1999, p. 52), the detailed features recorded for *Zenaspis?* sp. indet. by Gross (1961) are useful for comparison. What seems to be of particular value about the record of Estonian *Zenaspis?* sp. is the first appearance and restricted vertical distribution of this taxon, which agrees with the dating of Scanian osteostracan remains with *Zenaspis?*/*Hemicyclaspis* morphology. Some authors (e.g., Afanassieva, 1999, p. 122) regarded *Zenaspis?* sp. indet. of Gross (1961) as a synonym of *Waengsjoeaspis excellens* (Wängsjö). Early Devonian *Zenaspis* was placed by Janvier (1996) within the *Zenaspida* (Cornuata). Blicek & Janvier (1999, p. 89) included *Zenaspis* in the Lochkovian *Ctenaspis-Benneviaspis* Community from mainly grey-green, micaceous sandstones with red intercalations. The Late Ludlow Baltic '*Zenaspis?*' sp. remains, and the younger remains from German and Dutch erratics, were won by acid preparation from calcareous rocks, the Dutch remains from micaceous, arenaceous limestones that broke down easily.

The dentine ridges of the erratic Early Devonian Osteostraci gen. indet. form the top of a broad, sloping "Knochensocket" (= bone socle; Gross, 1961, text-fig. 18E), a feature unrecorded in *Zenaspis?* sp. indet. and in *Hemicyclaspis*, but possibly present (although sometimes less broad and depending on histological corroboration) in the Peyel material (Figs. 8, 9). According to Gross (1961) the ridges on these socles are twice as wide and high than those of *Zenaspis?* sp. indet., and the size of the vascular openings between them is c. 25 µm (*op. cit.*, p. 125), which differs from the size of the openings in P9059 and P9062 (Figs. 8, 9).

Morphological variation. Irrespective of identity, the following morphological variations have been found:—

- [I] Plates/scales with perforated external layer and 'longitudinal' arrangement of openings (= from 'anterior to posterior' or along 'longer axis' of fragment).
- [II] Plates/scales with 'longitudinal' ridges between which rows of openings are arranged. The ridges do not (or hardly) rise above the rest of the external surface. Interconnections between ridges occur.
- [III] Plates/scales with ridges that rise above the surrounding surface: a) ridges are low and close to each other and may be interconnected; or b) ridges are higher and more dispersed without interconnections, b1) ridges are mounted.

Within these variations several growth phases are evident and growth is also reflected by 'longitudinal' apposition of ridges or insertion of new ridges. The dimensions, shape, orientation and inclination of the ridges would seem greatest in variant [III]. Remains labelled hemicyclaspids comprise [I] and [II] plates and scales.

The plate fragments show differences in degree and position of basal curvature, for example, near the plate margins and in the middle (gable-like). These features are associated with position on the body. A marginal position on the trunk was suggested for the gable-like plate (Fig. 8). At least one, rectangular trunk (flank) scale was recognised (Fig. 6). For other scale forms it is harder or impossible to suggest a position on the body at present.

External apertures differ in size (per plate or scale fragment), shape (round, crescent-

like) and function (vascular-related, pore system-related). The apertures may be open, closed or partitioned (by sieve plates in the case of pores). In *Zenaspis?* sp. indet. pores were situated in shallow grooves between lateral extensions (connections) of the ridges in the superposition of the final ('secondary') dentine cover (Gross, 1961). I have insufficient exoskeletal indications from the hemicyclaspid remains to assume similar pore formation, whilst other osteostracan fragments unmistakably show such superposition (Fig. 2). This relation between pore system and superposition was not observed in Osteostraci indet. (Gross, 1961) or in, for example, *Tremataspis* (Gross, 1968). There are insufficient data on pores in my Scanian fragments to establish type of pore systems other than the *Zenaspis?* kind. Scanian (Pridolian or Whitcliffian) material might be referred to *Hemicyclaspis* rather than *Zenaspis?* when similar morphological features are shared without clear indications from 'secondary' dentine ridges, also because of the proximity of this genus, both in time and space. However, I think it is better to use hemicyclaspid instead of the genus name because of the uncertainties involved. Specimens with 'secondary', superposed dentine covers I refer to *zenaspid?* *sensu* Gross (1961).

Reappraisal of Ramsåsa H osteostracan remains in Vergoossen (2002a): P8828 (figs. 1, 2), hemicyclaspid; P8829 (figs. 3-5), compare in present paper with P9051 and P9106 (Figs. 5, 10 respectively).

Histology — Histological details are presently only available from a small fragment from Ramsåsa sample Q607 (Fig. 89), which morphologically resembles P8831 (Vergoossen, 2002a, figs. 6, 7) from Ramsåsa H. The ridge is made up of straight vertical tubules, which traverse several diagonal lines (ultrasculpture or growth lines?). Posteriad the tubules can follow a more oblique course, but the angle of inclination is not as sharp as that of the diagonal dividing lines. The round openings are presumably vascular.

Anaspid fishes; birkeniids

Loose scales; body of fish not known

Figs. 11, 12.

Remarks — The peculiar, eroded, low birkeniid scale fragment P9110 (Fig. 11) from the Peyel tube shows straight, elongate, tapering ridges that are shallowly folded medially (Fig. 11b) and split in their anterior part. The relatively coarse diagonal 'lateral ribs' on the ridges dominate any view. These 'ribs' do not reach the smooth ridge tops and are oriented posteriad. In places where the ridges seem to have eroded, series of successive chevron-like structures ('arrowheads') can be observed; their orientation and coarseness is the same as that of the 'lateral ribs.' The tops of the chevrons do not reach the height of the ridges. In all likelihood the 'lateral ribs' form the sides of the chevrons concealed in the ridges. The ridges slope slightly upwards posteriad and are arranged longitudinally (Fig. 11a), but not in obvious rows. Some ridges might originally have been longitudinally apposed. The width of the inter-ridge space varies and is wider or narrower than the greatest width of the ridges. Round apertures of the vascular system can be observed between the ridges and below the lower end of the

diagonal ribs or the chevrons. In longitudinal view (Fig. 11a) a single row of larger openings for the longitudinal canals can be seen just below the external surface. Dense bone makes up the rest of the scale; this is seen in the cross section (Fig. 11a), which also shows the low longitudinal visceral medial bar and the visceral groove in front of it. Bar and groove are minimally curved. Most of the overlapping crown area is probably missing; the posterior edge is concave and slightly projected over the medial bar. In longitudinal view (Fig. 11a) the scale is oriented to the right. P9110 represents a new taxon (*Ramsåsalepis* Blom *et al.*, 2003) with a feature (chevron-like ridge structures) especially typical of older birkeniid species.

The worn fragment P9125 (Fig. 12), from Ørvig's slides, differs considerably from the preceding scale, and has a rather wide, smooth and thin overlapped area. On the somewhat raised central crown platform there are diagonal rows of at least three, smooth and elongate, posteriad narrowing and shortening, triangular ridges. Many ridges are straight, some are curved. The sculpture is fairly closely packed, the intermediate space is about as wide as the width of the ridges. The overlapping crown area has broken off. The posterior neck is concave. The posterior basal margin has a rim (Fig. 12b). This fragment is reminiscent of birkeniid sp. E (with sculpture like water drops), from the Pridoli (*Poracanthodes punctatus* biozone) of the Ruhnu 500 core and of Ohesaare cliff, Estonia (Märss, 1986). Blom *et al.* (2002, p. 314) referred species E to *Liivilepis curvata*, together with 14 Scanian scales from the Öved Sandstone Formation from "one of several localities close to Ramsåsa Church." The distribution recorded for *L. curvata* ranged from the Late Ludlow (Tabuska Beds, Central Urals; Hamra Beds, Gotland) to Pridoli (Estonian and Swedish scales; age of the latter probably based on previous conodont and invertebrate datings). Another birkeniid from the same Ramsåsa locality, *Tahulalepis elongituberculata* (Blom *et al.*, 2002) of Late Ludlow or Pridoli age, was not observed in my material.

Thelodont fishes

Remarks — Thelodont scales figured and described in detail are from sample SW 32, unless stated otherwise.

***Thelodus* Agassiz, 1839**

Remarks — Among the *Thelodus* scales tested for their histology, no reclining dentinal tubules (as in *T. schmidtii*) were observed. The prominent and dense neck ribs of many *Thelodus* scales might have served to increase their attachment surface. Often, in scales from the body regions posterior to the head, the anterior base is thickened (cf. Vergoossen, 2002c, p. 80) and the anterolateral neck is smooth, whilst ribs are well-developed in the lateroposterior neck. Shape of anterior base (thickening or lengthening) and absence or presence of prominent neck ribs might be closely interconnected features. In some scale groups neck ribs are usually absent all around, as in, for example, forma *Thelodus trilobatus* specimens, which possess an extra attachment (anchoring) device in addition to Sharpey's fibres in the base, the median basal spur. The increase in attachment surface produced by prominent neck ribs need not be interpreted in terms of anchoring the scales, but could have contributed to the mobility of the scales when the

ribbed surface was in touch with the elastic fibres in the corium. In this case, the latero-posterior prominence of the neck ribs might be bound up with greater flexibility for (propulsory) motion towards or away from the caudal region.

The variable size of the basal opening, or the closing of this opening in *Thelodus sculptilis* scales in the 0.106 fraction demonstrate that several growth phases are represented in these minute scales. Histological tests, to establish variability in number of growth lamellae in crown or base, failed.

Squamation of a hypothetical *Thelodus parvidens* fish body Some scale form groups

Figs. 13-21.

Glabrous, cephalopectoral scales (Figs 13-15). *Thelodus parvidens* Agassiz, 1839, *sensu Vergoossen (2002c)* — Sample SW 14 yielded one twinned scale. The specimens are fused on one side of the crown and base (T, Table 2). In sample SW 15 the smallest, smooth *T. parvidens*-like crowns have often lost their lustre, indicating that their upper surface was affected by erosion, which can make it difficult to establish whether they were smooth originally. This, together with the general shape of some of these scales (e.g., crown width smaller than basal width, which is not characteristic of *parvidens*), makes their determination as *T. parvidens* uncertain and several of this type are referred to *T. sculptilis* (cf. Vergoossen, 2002a, fig. 19). The uncertainty is increased by the observation that only when light is applied to the surface in a skimming fashion, other scales show regular but very weak, radial longitudinal striation on the crown; these scales are referred to forma *T. radiosus*. The relief of the ridges and folds in the crowns of forma *T. radiosus* scales can be very weak in all fractions of all samples (Figs. 30, 31). Again, to which extent this condition reflects original state or results from erosion needs to be further investigated. At least some erosion can be demonstrated in many specimens, although the degree varies.

In few scales from sample SW 32 the glabrous crowns possess double posterolateral crown rims (Fig. 13), a feature also occurring in glabrous crowns (Fig. 14) in a Pridoli fauna (*'Poracanthodes punctatus zone'*) from a Dutch erratic (Vergoossen, 1999a). The double rim begins round the lateral corners of the crown. Width of the area between the rims varies from *c.* 18-31 μm in P9136 (Fig. 13) and from *c.* 30-40 μm in RGM 323079 (Fig. 14). In another scale, P9143 (Fig. 15), this area widens from *c.* 18 to 40 μm posteriad; here, the effect of a lowered lateroposterior crown margin is created, as known from *Thelodus laevis* (Märss, 1986, pl. 17; Gross, 1968, fig. 1c) or *Thelodus carinatus* (Märss, 1986, pl. 18). The specimen is also reminiscent of scales with anteriorly ridged crowns, and lowered lateroposterior (partim spinose) crown margins, assigned to *T. carinatus* (Vergoossen, 2002c, figs 64, 68, 69; Ramsåsa D); similar scales, which might belong to a new taxon, were not observed in the Ramsåsa E faunas. Neck rib density per 0.1 mm in figured scales: *c.* three to four (P9136), *c.* three (RGM 323079), increasing from *c.* four (anterior) to six (midposterior) in P9143. A double rim also occurs in a scale (P8835) from Ramsåsa H (Vergoossen, 2002a, fig. 13). Histological data are not available. Recently, a double rim was suggested in drawings of the crown of *T. calvus* (Wenlock-Ludlow?, Severnaya Zemlya Archipelago; Märss & Karatajute-Talimaa, 2002, fig. 14). The photographs do not show the feature (*op. cit.*, fig. 5), which was not mentioned in the description.

Tricuspid glabrous scale (Fig. 16) — Only specimen P9144 is an eroded scale with postero-incised tricuspid crown, the median cusp being largest. It differs in several respects from tricuspid glabrous crowns known from Ramsåsa D (Vergoossen, 2002c, figs. 33-36); the crown is flat and has a conspicuous lateral overhang, as in a “worn, seemingly glabrous *Thelodus* scale,” and a calcarate glabrous scale (Vergoossen, 2002c, figs. 42a, 28a, respectively). It also shares with the latter scale a square anterior neck and the flatness of the crown.

Rhizoid scale (Fig. 17) — Only specimen P 9145 is a scale with a smooth, convex crown that has a spinose posterolateral rim on one side. Neck all around, with vertical lateroposterior neck ribs (density *c.* five per 0.1 mm). The base widens out and thickens anteriorly, where it is lumpy (initial rhizoid phase). Compare with a ‘variant 1’ scale from Ramsåsa D (Vergoossen, 2002c, fig. 32; the thin base in this scale is not thickened anteriorly).

Currently, there is insufficient material for a proper taxonomical or preservational assessment of the forms discussed above.

Polycuspid forma Thelodus trilobatus Hoppe, 1931 (Figs 18-20) (included in *Thelodus parvidens* Agassiz, 1839 *sensu* Märss, 1986) and spurred glabrous scales (Fig. 21) — Märss & Miller (2002) recently re-instated *T. trilobatus* Hoppe as a separate species for scales from a sample from the Welsh Borderland, placing diverse form groups within a *T. trilobatus* body zonation scheme. Some of the variants included in their new scheme (pers. obs.) were first described and figured from Öved Sandstone material (Vergoossen, 2002c). In my opinion this scheme groups together heterogeneous scales and for this reason their interpretation is not followed herein.

P9146 (Fig. 18) and P9147 (Fig. 19) are conventional polycuspid scales, the latter with a more asymmetric tendency to the right (in posterior view), of one crown half and of the anterior basal thickening. Some of their features are compared below.

	P 9146	P 9147
Crown	Eight, slender cusps, with polygonal cross section. Lateralmost cusps smooth; three on the right (in posterior view), two on the left. Median ridge pair ascending from very low anterior neck. Median ridge pair converging in midposterior ridge and continuing as one ridge. Straight ridges in cusps in midcusp ridges position and parallel. Ridges on cusps flanking median cusp blunted anteriorly, or even fading.	Seven, mostly wide cusps. Idem; two or three on the right, two on the left. Median ridge pair slightly protruding forward, on higher anterior neck. Median ridge pair ends before midposterior cusps, one ridge ends at deepest incision of posterior crown. Ridges in cusps in lateral position, and diverging posteriorly; the surface of the largest cusps is chiefly smooth. All ridges sharp-edged.
Base	Slender anteromedian basal spur, projected forward and only slightly inclined ventrad.	Anteromedian stub slightly tending to the right.

P9146 is from a position on the body closer to the midline, and has a more delicate crown of which both the anterior crown part and the posterior cusps played a different role in channelling and dividing the water current (at the hydrodynamic micro level). It remains to be proven whether position (in one individual) is enough to explain such functionally-related morphological differences, even if it is assumed that the scales derive from the same taxon.

P9148 (Fig. 20) may show form grading of a smooth-crowned scale to a polycuspid trilobatiform scale of either a *T. parvidens* or *T. sculptilis* fish. The greater part of the crown (left and central in Fig. 20a) is smooth and convex; anteriorly, the crown bends over the neck. The smooth part has a posterior cusp in mid crown position; it is the largest cusp. Probably there was a second cusp on the smooth part (to the right, Fig. 20c). One lateral crown half has a ridged and tricuspid lobe; the ridge ends in the largest cusp of the lobe (Fig. 20c). The lobe is separated from the smooth crown area by a suture and a narrow posterior groove. At least one faint furrow is visible in the smooth part, parallel to the groove that bounds the lobe. The neck has lateroposterior vertical riblets. Anterolateral base much thickened and deepened ventrad compared to posterior base (Fig. 20b) and projected forward medially. This specimen shows little resemblance to spurred glabrous scale P9156 (Fig. 28), to tricuspid glabrous scale P9144 (Fig. 16) or to a variant 3 specimen (spurred glabrous polycuspid, Fig. 21) from Ramsåsa sample Q607.

Monocuspid 'trilobatus' scales — The two scales of forma *Theلودus clavaeformis* Lehman, 1937 (sample SW 15, Table 3; sample SW 32, Table 4; cf. Vergoossen, 1999b, p. 272) are one sieve fraction bigger than the dimensions given by Lehman (1937, p. 94). Another monocuspid 'trilobatus' scale, from Helvetesgraven (Fig. 91), shows dentinal tubules entering the pulp cavity; some of the tubules in the middle curve anteriorly in their lower part and continue down straight from the curve. Posteriorly the tubules are straight, oblique and longest. Sharpey's fibre spaces can be seen in the anterior end of the basal spur.

Squamation of a hypothetical *Theلودus sculptilis* fish body Some scale form groups

***Theلودus sculptilis* Gross, 1967**

Figs. 22-27; 28, 29?; 32-34.

Remarks — In the 0.106 fraction some variants were not observed. This particularly concerns scales with many crown folds and ridges as illustrated by Märss (1986, text-figs. 21:15-17; 22:18, 19) from body zone III. Such ornament may be restricted to bigger scales.

Oral scales (Figs. 22-24), *oral?* (Fig. 25) — P9150 (Fig. 22) has a slender, midposterior crown peg projecting over neck and base, and with a dorsal ridge; in lateral view it looks like a keel. Neck higher posteriorly than anteriorly. Vertical well-expressed longer and shorter lateroposterior neck ribs, density c. 4-5 per 0.1 mm. Low basal rim. Compare with Vergoossen (2002c, fig. 52; this scale has, for instance, fewer, non-bifurcating ridges and no basal rim).

Table 4. *Thelodont* fishes from Ramsåsa E, sample SW32 (selection). Taxa $\geq 5\%$ in bold.

Fraction	0.106	0.212	0.355	0.425	0.5	Total	% TT
Number of taxa: 17 ⁽¹⁾ not counted	9	15	8	9	8		
<i>Thelodus parvidens</i> s.s.*	40	221	97	180	138	676	50.9
forma <i>T. costatus</i> *				1		1	0.08
head scales		6	1	3	1	11	0.8
forma <i>Thelodus bicostatus</i>		13	1			14	1.1
forma <i>Thelodus trilobatus</i>							
multicuspid	19 [3B]	54 [23B]	9 [4B]	7 [2B]	2	91 [32B]	6.8
monocuspid	2					2	0.15
forma <i>Thelodus clavaeformis</i>							
Lehman, 1937		1				1	0.08
variant 1*	1	1				2	0.15
variant 2*		1	1		1	3	0.23
variant 3*		1				1	0.08
<i>Thelodus traquairi</i>	1	20	9	11	4	45	3.4
<i>Thelodus</i> sp. indet., forma <i>baltica</i>		4		1		5	0.4
<i>Thelodus sculptilis</i>	100	71	51	44	22	288	21.7
forma <i>Thelodus radiosus</i>	18	34	14	15	12	93	7
<i>Thelodus sculptilis</i> or <i>T. parvidens</i> sensu Märss, 1986 ⁽¹⁾	3	25	10		1	39	2.9
<i>Thelodus</i> sp. indet., forma <i>subulata</i>	21	4				25	1.9
<i>Thelodus</i> sp. indet., diverse forms	10	17		2	3	32	2.4
Total <i>thelodont</i> fishes	215	473	193	264	184	1329	
% of 1329	16.3	35.9	14.6	20	13.9		

Oblong scale P9151 (Fig. 23) can be compared well with more ellipsoid cephalopectoral specimen P9154 (Fig. 26). The anteromedian crown has been further constricted in the first (Fig. 23a), whose crown rims are ridged (Fig. 23b). The constriction of the midposterior surface is more prominent in the second (Fig. 26), which has sinuous crown rims. There are *c.* four vertical lateroposterior neck ribs per 0.1 mm.

P9153 (Fig. 25; Peyel residue) lacks the sharp anterolateral crown ridges of P9150 (Fig. 22), but has a faint midposterior ridge in the slender midposterior three-forked crown point, which is strongly twisted to the right. Short and long, mostly vertical neck ribs, all around, *c.* three per 0.1 mm. The base is not thickened anteriorly.

Cephalopectoral scales (Figs. 26-29, 33) — P9155 (Fig. 27; only specimen known) has a predominantly smooth crown, but the ridging on one side (the left in posterior view) indicates form grading from or to oral scale types.

The crown of P9157 (only specimen; Fig. 29) is triangular, projects over neck and base lateroposteriorly, and is both longitudinally and latitudinally curved, mostly in its anterior part, which bends ventrad. Two shallow grooves mark off the anteromedian crown part (a sculptiliform feature) and fade out half way along the crown. The straight anterior crown rim slightly recedes before the grooves (Fig. 29a). The neck makes up *c.* one third of scale height and has faint vertical ribs. The anteromedian base has a median constriction, projects well forward of crown and is directed ventrad. Latero-

posterior base broken. Compare with a scale with a more convex anterior crown and no forward projection of base (Vergoossen, 2003b, fig. 31).

Calcarate, glabrous scale P9156 (Fig. 28; only specimen) resembles one from Ramsåsa D ('*T. parvidens* s.s., variant 1,' Vergoossen, 2002c, fig. 31). The midanterior crown is more prominent because the lateral parts of the anterior crown rim have receded farther posteriad. This sculptiliform feature is weakly expressed; the scale is also not typical *T. parvidens*. A calcarate, glabrous specimen from Helvetesgraven (Fig. 90) has posterior neck ribs and shows a *parvidens* type of histology, with the dentinal tubules probably postmortally widened.

Postpectoral (Figs. 32, 34?) — The crown of P9160 has a midposterior peg (Fig. 32a; hardly visible in posterior view, Fig. 32b), but is remarkable for its lower central section between higher lateral wings that make an obtuse angle with the base and spread outwards steeply (Fig. 32a). The base thickens greatly anteriad (compared to its posterior thickness) and has a midanterior constriction.

Basal features (Figs. 33, 34) — P9161 (Fig. 33) has a regularly sinuous anterolateral basal outline. The rhomboid low base P9162 (Fig. 34) has symmetrically sinuous anterolateral margins, with a midanterior point (Fig. 34b). The anterior basal half (Fig. 34a) is a bit concave, in contrast to the flat posterior part.

Radiosiform scales (*Thelodus radiosus* Lehman, 1937, *sensu* Vergoossen, 2003b)

Figs. 30, 31.

Cephalopectoral — Some scales can hardly be distinguished from glabrous *T. parvidens* s.s. specimens. One such scale (Fig. 30) was selected for its fine longitudinal striation on the crown. The striation had been observed with light applied to the surface in a skimming fashion and using a binocular microscope. However, the SEM could not bring out the relief. P9159 (Fig. 31) is more elongate, and in the posterior crown half, the central crown area is lower than the crown sides (Fig. 31b). Neck rib density *c.* four per 0.1 mm. Scales can exhibit shallow crown grooves which do not reach the anterior crown rim; the neck ribs in such specimens are sharp.

Squamation of a hypothetical *Thelodus traquairi* fish body

Some scale form groups

Figs. 35-39; 40?, 41.

***Thelodus traquairi* Gross, 1967, and *Thelodus* sp. indet., *subulate* forms**

Conventional morphology (Fig. 35) — In some scales (not figured), the anterolateral radial ridges on the more or less erect crown can be swollen or thickened (almost like tiny beads) in their proximal part, i.e., where the ridges rise from the neck (if present).

The lateroposterior base is shallowly grooved in P9163 (sample SW 15, Fig. 35), producing basal 'lumps.' The initially rhizoid lumps are associated with and situated below neck ribs (Fig. 35a). Anteriorly, where neck ribs are absent, basal lumps

are also absent. The visceral surface of the base is concave, widening out from the narrow central pulp opening.

Ramosiform morphology (Fig. 36) — P9164 (Fig. 36) has no anterior neck, *c.* four posterior neck ribs per 0.1 mm and a smooth ventral crown surface. Ramosiform scales are extremely rare (one specimen) in the Ramsåsa E samples; they were less rare in the Ramsåsa C sample (Vergoossen, 2003b).

Remarks on subulate morphology — Scales that illustrate the transition from typical *T. traquairi* to slender, small forms supposedly from the pinnal or posterior body regions (Vergoossen, 2002a) occur in the present material, chiefly in the 0.106 fraction, and are here assigned to forma *subulata*. The name refers to the slender, awl-like shape of the crown. The scales are discussed below, together with associated variants from the same sample that might lead on to them, and irrespective of the species to which they might belong. Currently it is not clear whether this morphology is a new small *Thelodus* taxon or represents a particular body variant of one of the known *Thelodus* species from the *T. sculptilis* zone, in particular *T. traquairi*, because form grading to this species occurs most and is best demonstrable. However, I have observed subulate scales in undescribed Baltic *T. sculptilis* assemblages (e.g., from Varbla, Estonia; Figs. 93, 94) without *T. traquairi*, whereas one rich and intriguing Ramsåsa fauna (Q607; Vergoossen, 2003a, chapter 6) with relatively few *T. sculptilis* and *T. traquairi* scales, has so far not yielded *subulata* scales in the 0.106 fraction, which abounds in scales.

***Thelodus* sp. indet., forma *subulata*, new form**

Figs. 37-39.

Diagnosis — Minute scales (chiefly from 0.106 mm sieve fraction) with slender, subulate, posteriad inclined and tapering crowns that have a median ridge pair converging posteriad and with intermediate fold. Crown can have a sharp, midventral keel. Crown rims (with or without lateral rim pair) and median ridge pair anteriad constricted. Low to very low anterior neck; posterior neck higher and usually with vertical neck ribs. Very low, subrounded base with basal rim and with or without midanterior constriction or indication of short spur. Midventral pulp cavity into which straight dentinal tubules coalesce.

Synonymy — Ramsåsa H, *Thelodus traquairi* (Vergoossen, 2002a, figs. 8, 9, 39-43, 47-50, 54); Ramsåsa C, subulate forms (Vergoossen, 2003b).

Number of scales from Ramsåsa E — See Tables 1-4.

Typical specimens — P8831, P8832, P8848, P8849, P8852 from Ramsåsa H; P9165, Ramsåsa E.

Distribution — Upper Ludlow, *T. sculptilis* biozone, Ramsåsa C, E, H, Öved Sandstone Formation.

Descriptions — P9165 (Fig. 37) has a very narrow median fold and the median ridge pair is almost reduced to a single ridge (Fig. 37a). Angle of inclination *c.* 120°.

P9166 (Fig. 38) looks very similar to the Ramsåsa H specimens (see above); slender, elongate, inclined crown (angle of inclination *c.* 110°) with median raised ridge pair and intermediate shallow fold. Near the top, ultrasculpture of longitudinal parallel striations (Fig. 38b) occurs on the ventral crown (comparable to that on P9180; Fig. 52b). Such ultrasculpture was also observed in a scale from Ramsåsa H (Vergoossen, 2002a, fig. 42).

P9167 (Fig. 39) is more strongly geniculate, has a rather high anterior neck and a short midanterior basal projection.

Two scales from the Varbla 502 core, depth 19.10 m (Upper Ludlow, Tahula Beds, lowermost *T. sculptilis* zone), Estonia, are morphologically similar to those from Ramsåsa. Their histological structure is seen in Figures 93, 94. Depending on the view, the orientation of the tubules may differ. In anterior crown view (Fig. 94) tubules in the anterior crown half tend to curve anteriad in their lower reach; a few are s-shaped. Seen in posterior view and focusing on the basal opening (Fig. 93), the tubules bend laterad. The tubules coalescing into the narrowing pulp cavity further posteriorly are straight and longest. In both scales the base is very thin.

Remarks — Form grading between P9165 scale and a spurred specimen from Ramsåsa H (Vergoossen, 2002a, figs 26, 27) is conceivable.

***Theلودus* sp., with traquairi morphology?**

Fig. 40.

Remarks — Damaged, geniculate, traquairiform and sole specimen P9168 differs from the subulate Ramsåsa H scales, but is still close to them and larger. A short anteromedian ridge pair protrudes anteriad from a low neck (Fig. 40b) and is inclined rather steeply posteriad. Where the ridge pair converges to form a single median ridge there is an abrupt curve (*c.* 135°; Fig. 40b) to almost horizontal. The anteromedian crown is prominent; such a feature is not rare in *T. traquairi* scales from Ramsåsa (pers. obs.; cf. Gross, 1967, pl. 4, fig. 11a, where the expression of the feature is weaker). The posterior crown point is beak-like (Fig. 40b, c). In the posterior third of the crown, one lateral crown rim branches anteriad. Neck all around and unstricted. *Circa* five, long and short vertical posterior neck ribs per 0.1 mm.

P9169 (Fig. 41; sole specimen) is a *T. traquairi* specimen with affinity to the preceding scale in the prominence of its anteromedian crown pair, which has taken the shape of a separate, forward projected (Fig. 41b), raised (Fig. 41c) miniature crown. Neck rib density *c.* four per 0.1 mm.

Body of fish not known; more scale form groups

Figs. 42-53.

***Theلودus* sp. indet., forma baltica and P9171**

Figs. 42, 43.

Remarks — In anterior view (Fig. 42a), P9170 resembles a forma *baltica* scale from Ramsåsa C (Vergoossen, 2003b, fig. 63a), but the present crown has more lateral

ridges. The intermediate folds are not deep enough for the ridges to stand out thin and sheet-like. The crown is also more sculptiform and does not project over the base posteriorly (cf. Fig. 42b; Vergoossen, 2003b, fig. 63b). There is a distinct upper basal rim. The base is thickened anteriorly, has a midanterior constriction (but no spur), and is steeper (nearly vertical) midanteriorly (S. Turner, pers. comm: *T. sculptilis*, *T. goebeli*).

Postpectoral? scale P9171 resembles scales from a morphoserries (including forma *baltica*) described from Ramsåsa C with radially ridged crowns broader than long, with bulgy midanterior base and assigned to *T. traquairi* (e.g., Vergoossen, 2003b, fig. 61), although some scales also show sculptiform features. In P9171 the characteristic sculptiform midanterior pair of crown folds is absent, but the scale is also not typical of *T. traquairi*. The median ridge pair converges in the posterior crown and has hardly any prominence (Fig. 43b, c); the pair is flanked by two radial ridges in one crown half and by one ridge in the other (Fig. 43b, c). All ridges extend roughly equally far posteriorly. The folds between the ridges are not deep enough to produce 'sheets' or 'wings' (Fig. 43c) and this feature is only weakly expressed (Fig. 43a,b). The neck is low with faint ribs.

Thelodus sp. indet., diverse scale types

Figs. 44-52.

Oral? scale — P9172 (only specimen) has a square shape (Fig. 44a). The crown tends to become conical (Fig. 44b), steeper posteriorly than anteriorly, and shows a mixture of densely packed, low radial ridges and posteriad converging ridge pairs of which the longest end distally in the peg-like crown top (Fig. 44a). This top is situated in the posterior crown half, between the scale centre and the posterior crown margin (Fig. 44a). In the Ramsåsa E faunas, the peg is a sculptiform feature, but the overall appearance of the crown is unlike that of *T. sculptilis* scales known from the literature. The ridges are steeper and shorter posterolaterally than anterolaterally and the intermediate folds are very shallow. The neck is slightly higher than the base. There are *circa* four to five strongly eroded neck ribs per 0.1 mm.

Cephalopectoral scale of forma bifrontis, new form, and scales previously assigned to T. carinatus (Vergoossen, 2002c) — The 'transitional', convex crown of P9173 (Fig. 45; sole specimen) is truly a Janus face, with oral and cephalopectoral features. It has an anterolaterally ridged triangular area, more or less sculptiform in appearance. The point of the triangle, situated in the posterior crown half, is the highest scale part. The greater part of the crown, i.e., lateral and posterior to the triangle, is smooth and slopes ventrad. The lateroposterior crown has two distinct notches, one on each side. The anteromedian crown has paired ridges converging posteriad and with a shallow intermediate fold. This crown type resembles scales identified as *T. carinatus* (Vergoossen, 2002c, figs. 64b, 67, 68), one of the differences being the flat rather than sharp ridge tops. Despite the differences, these scales and similar forms from Ramsåsa sample Q607 might perhaps be grouped together in a new *Thelodus* taxon, either sculptiform or with a mixture of morphological features from several species. The issue cannot be resolved here and this scale type is provisionally called 'forma *bifrontis*' (= with two faces, referring to the crown morphology). Vertical neck with vertical ribs (density *c.*

four per 0.1 mm). Neck and base equally high, between c. 40-50% of total scale height. Base rhombic, with upper basal rim (S. Turner, pers. comm.; *T. sculptilis*, *T. goebeli*).

More Janus faces. Cephalopectoral, antero-incised glabrous (Fig. 46) and latero-incised glabrous (Fig. 47) — P9174 (sole specimen; Fig. 46) is roughly as wide as long. The crown is angular anteriorly and markedly straight posteriorly; the anterior margin bends rather strongly ventrad (Fig. 46b). The forward projected, short anteromedian ridge pair converges approximately at the level where the flanking ridges begin and continues posteriad as a single median ridge for a short stretch. The space between the ridge pair is flat. There are three short radial ridges on each side of the median pair in the anterior crown half; the posterior crown half has no ridges. The posterior crown rim is a bit shorter than, and parallel to, the latitudinal axis of the scale. The crown is smooth posterior to the ridges and has a slight midposterior notch. The ridges rise abcentro from the upper neck, and curve centrad abruptly and at right angles after c. 0.05 mm. Vertical neck ribs all around and more prominent in the posterior neck; density c. six per 0.1 mm anteriorly. Neck and base make up half the scale height, neck c. twice the height of base. Upper basal rim all around. The base has a slight midposterior notch under the crown notch, and a slight anteromedian constriction. This scale may be sculptiliform. It is comparable to *T. sculptilis* from the Tahula Beds (Märss, 1986, text-fig. 21:19; this scale is longer than wide and has a median longitudinal crown ridge); from the Ramsåsa Bed (*op. cit.*, text-fig. 22:9, 13; these scales are both longer than wide, the latter has a posterior peg); and *T. parvidens*, Vergoossen (2002c, figs. 23, 27) from Ramsåsa D.

P9174 differs from *bifrontis* scales in that the two different crown parts do not meet at a distinctly higher, more or less central scale point (= posterior crown point lifted and shifted centrad, which is a feature of oral scales), because the crown is too flat.

Sole specimen P9175 (Fig. 47) resembles the preceding scale, with form-grading typical of oral to cephalopectoral. It is longer than wide, with all the ridges in one lateral crown half (to the right of the anteromedian and anteriad widest ridge; Fig. 47b). The four longest ridges radiate towards the highest, central crown part (as in forma *bifrontis*). There are two shorter intermediate ridges. The deepest notch in the crown is to the left of the anteromedian ridge (Fig. 47b) and on that side further weak folding occurs (Fig. 47a). Neck base transition is unclear. The basal outline is more or less round. The crown margin to the left of the anteromedian ridge was magnified 2000 times. This vertical section shows extremely fine, dense, parallel, horizontal and probably incremental layering (Fig. 47c), which, however, cannot be interpreted as the 'ordinary' (much coarser) growth zones within the crown dentine. Too little high resolution scanning has been done on well-preserved thelodont and acanthodian scales for comparisons to be made.

Other antero-incised glabrous, cephalopectoral scales (Figs. 48-50) — At first sight P9176 (sole specimen) (Fig. 48) seems very similar to a scale (sole specimen) from Ramsåsa D (Vergoossen, 2002c, fig. 75), but there are minor differences; the shape of the crown is more rhomboid and not so slender anteriorly, the median crown ridge is not so well-developed, the anterolateral lobes have deeper intermediate notches and folds and extend further medially. The anterior crown is not flattened and has a rim with small bead-like lumps (Fig. 48a) and shallow intermediate notches. The vertical neck is better preserved, with long and short neck ribs nearly all around; only the most anterior

neck part seems rib-free. The most robust ribs were observed posteriorly. Density *c.* five to eight per 0.1 mm. Neck and base about equally high and together making up *c.* half the total scale height (cf. also Vergoossen, 2003b, fig. 9, *Thelodus parvidens*).

Sculptiliform? scale P9177 (Fig. 49; sole specimen) has a triangular crown that is round anteriorly and oriented horizontally. Despite the eroded state of the scale, the regularly sinuous posterolateral crown rims are interpreted as original. The anterior crown rim is lobed; the median lobe is most prominent and largest. The intermediate grooves are narrow and shallow. Lobes and grooves occupy *c.* one-third of the crown length. The crown does not extend over base, but projects over neck all around. Faint posterior neck ribbing (Fig. 49a). Neck and base are about equally high. An upper basal rim marks the transition from neck to base.

Sole and small specimen P9178 (Fig. 50), sample SW 15, has a symmetric, triangular, slightly convex crown that curves ventrad anteriorly and with two short, sharp midanterior ridges parallel to the longitudinal axis of the crown and to each other. The ridges rise over the surrounding crown surface and the intermediate fold is shallow and fades out slightly further posteriorly than the ridges. Crown overhang is marginal. The neck makes up the largest part of the height of the scale and bears *c.* four vertical riblets per 0.1 mm lateroposteriorly. Base low and flat, basal outline follows crown outline.

Pinnal scales? (Figs. 51, 52) — P9179 (Fig. 51) looks like a subulate scale in lateral view (Fig. 51b), but in anterior view (Fig. 51a) it differs (cf. Figs. 37-39) because it has an anterior crown rim. From the anterolateral corners of the low, ellipsoid base, the upper basal rim ascends to midanterior (Fig. 51b), where the base is thickened.

In P9180 (Fig. 52) the anterior crown rim sticks out slightly further forwards anteromedially (Fig. 52a). The crown is horizontal and the crown folds are very shallow (Fig. 52a). The neck has *c.* four, well-developed ribs per 0.1 mm anteroposteriorly and the base is thin. There is a short rim below and parallel to the crown rim (Fig. 52a). From the posterior end of the lower rim to the crown point, ultrasculpture of fine, low-angled oblique, longitudinal, parallel striae can be observed (Fig. 52b). These may reflect the course of the dentinal tubules.

Note — A comprehensive survey of ultrasculptures is needed, as various patterns in various taxa might reflect different microstructural features or serve various functions (cf. Vergoossen, 2003b, on osteostracan ridges, 'mechanical load;' Märss, 1999, p. 1088, on thelodont crowns, 'mucus anchor'). Detailed data per species on pattern and spacing of vertical microstriae on the surface of conodont elements from Skåne were given by Jeppsson (1974). The reticulate patterns on the forecrown of *Thelodus laevis* (Gross, 1967, p. 16) and *Thelodus* sp. (Fredholm, 1988a, fig. 7H, I) are reminiscent of cell imprints on conodont elements (Dzik, 2000, fig. 4) and of 'ectodermal pits' on the crowns of recent shark scales (Reif, 1985, pp 16-18).

Indeterminable thelodont scale

Fig. 53.

Remarks — In sample SW 15, the tiny, cruciform scale P9181 is one of two specimens

looking like an oral *Loganellia* scale; this needs histological corroboration since only one additional, doubtful loganellid scale was recovered from the Ramsåsa E samples (SW 15; Table 3). This cruciform morph might also grade to tiny, oral *Thelodus* scales assigned to *Thelodus traquairi* (Vergoossen, 2002c, fig. 55). Unlike the latter, the present scale has no neck and does not taper distad. Three of the ridges forming the cross bifurcate anteriorly, one trifurcates. The very thin, disc-like base is open in the centre on the visceral side.

Acanthodian fishes

Remarks — All the acanthodian remains figured and described in detail are from the Peyel tube, unless stated otherwise.

Genus *Nostolepis* Pander, 1856 sensu Gross, 1947, 1957, 1971

Remarks — The lack of information on basic *Nostolepis* histological features (e.g., network of vascular canals, Stranggewebe, bone cell lacunae) in the Ramsåsa (E) scales is a handicap to the definite identification of these scales.

Squamation and other bony elements of a hypothetical *Nostolepis striata* fish body; some scale, spine and tooth plate form groups

***Nostolepis striata* Pander, 1856 sensu Gross, 1947, 1957, 1971**

Figs. 54-80.

Remarks — Since all the remains from the Ramsåsa E samples identified, described, and figured in this section as *Nostolepis* can be linked with a scleritome *Nostolepis striata*, I have opted to group them together in this paper under this name. For example, slender, elongate, small scales of the 'elegans' and cf. *N. minima* morphs might derive from the fin webs or spinal plates (cf. Fig. 79) of a *N. striata* fish. Although I regard *N. striata* as a 'bucket' name, I have at the same time begun to document morphological features that might help distinguish *N. striata* scales of the Öved Sandstone Formation from others. With histological data lacking, stellate and umbellate scales (Tables 5-8) might also derive from gomphonchids in the faunas, but have been grouped with *N. striata* in the tables.

The description, analysis and assessment of the morphology of *Nostolepis striata* trunk and topospecific scales in order to draw up a check list of characters (Vergoossen, 2002b, c, 2003b; Appendix) is continued. In this paper the focus is on big and 'modified' trunk scales (> 0.5 mm), plus small *N. minima*-like scales.

Nostolepis minima Valiukevicius, 1994, was proposed as an acanthodian zonal fossil for the lower part of the Lochkovian in the East Baltic and Russia by Valiukevicius (2000), and for the Old Red Sandstone Continent (Blieck & Turner, 2000). Vergoossen (2002a, figs. 58, 59, 62, 63) figured and discussed morphologically similar scales without lateral crown rims (identified as *N. striata*) from Ramsåsa H, and with lateral crown rims (2002c, figs. 94-99, 'forma elegans') from Ramsåsa D. These scales are larger than the ones from Ramsåsa E (see below and Tables 5-7). The resemblance to the zonal

Table 5. Acanthodian fishes from Ramsåsa E, sample SW 14 (fully picked). Taxa $\geq 5\%$ in bold.

						Total	% AcT
Fraction	0.106	0.212	0.355	0.425	0.5		
Number of taxa: 10	5	7	2	4	5		
<i>Nostolepis striata</i>	14	18	3	1	7	43	40.2
forma ' <i>elegans</i> '					2	2	1.9
forma ' <i>Nostolepis minima</i> '		7				7	6.5
stellate plates <i>sensu</i> Gross, 1971				2 [1F]	2 F	4	3.7
<i>Gomphonchus sandelensis</i>	1	2				3	2.8
<i>Gomphonchus volborthi</i>	5	15	3	2	8	33	30.8
gomphonchid scales		2				2	1.9
poracanthodid scales	2	1				3	2.8
indeterminable acanthodian platelet	1					1	0.9
indeterminable acanthodian spines F		1		2	6	9	8.4
Total	23	46	6	7	25	107	
% of 107	21.5	43	5.6	6.5	23.4		

fossil concerns the morphology of particular specimens (Valiukevicius, 1994, figs. 11, 12; 1998, figs. 7, 8) and similar, unfigured material (Valiukevicius, pers. comm., Gross Symposium, Göttingen, 1993). The trunk scales of *N. minima* are considered closely allied to the *N. striata* scale group (Vergoossen, 2002b).

Big scales (> 0.5 mm) were only obtained from the Peyel residue and Ørvig's slides. Many of these are 'modified trunk' scales, differing remarkably in several constant features from the small trunk scales I have dealt with hitherto. Full treatment of this subject is outside the scope of the present paper, but an attempt has been made to work out some of the differences.

The *N. striata* scales in the 0.106-0.212 fractions have flat to moderately convex bases, which may imply that several growth phases are represented among these minute scales, not just the youngest; body position is another factor influencing basal depth. Only few scales have flat bases.

Nostolepis minima-like trunk scales (Figs. 54, 55) and scales of forma *elegans*. Descriptions (1) — *Nostolepis minima*-like scales occur especially in the small fractions and SW 15 (0.106-0.212; Table 6), and, distinctly fewer, in larger fractions (SW 32; Table 7). The Scanian scales may be smaller than the common size range (0.2-0.45 mm, Valiukevicius, 1994, p. 160). They may resemble small specimens of the '*elegans*' form group (Vergoossen, 2002c, figs. 94-99; 2003b) or rare monotubercular platelets (Vergoossen, 2002c, figs. 100, 101). Their morphological plan of construction is uniform and 'simple;' the *N. minima* scales from the East Baltic and Byelorussia (Valiukevicius, 1998, pl. 1, figs. 5-9) show greater variety. The crown is triangular and contained within the rhomboid base, except the posterior point, which may jut out. Usually a pair of lateral crown ledges (one ledge on each side of the crown and beginning near the latitudinal axis of the scale) converges at or near the tip. There is one short anteromedian crown rib, exactly on the longitudinal axis of the scale, or a rib pair, parallel to this axis. The ribs usually fade out before the latitudinal axis of the scale. The median crown surface is depressed and the crown rims bend inwards anteriorly. The inclination of the crown

Table 6. Acanthodian fishes from Ramsåsa E, sample SW 15 (selection). Taxa $\geq 5\%$ in bold.

Fraction	0.106	0.212	0.355	0.425	0.5	Total	% AcT
Number of taxa: 21	9	15	13	7	8		
<i>Nostolepis striata</i>	31	43	15	17	22	129	40.1
forma ' <i>elegans</i> '		2				2	0.6
forma ' <i>Nostolepis minima</i> '	14	24	2			40	12.4
squamae proniae		1			1	2	0.6
coronate scales & plates	1	2	1		4	1.2	
stellate plates <i>sensu</i> Gross, 1971		2			1	3	0.9
squamae umbellatae <i>sensu</i> Gross, 1971 F		2		1	2	5	1.6
spines F					1	1	0.3
<i>Gomphonchus sandelensis</i>	3	8	1	6		18	5.6
<i>Gomphonchus volborthi</i>	17	26	4	17	8	72	22.4
<i>Poracanthodes? lehmani</i>			1			1	0.3
punctatiform cf. <i>Poracanthodes</i> <i>punctatus</i>		1				1	0.3
<i>Radioporacanthodes biblicus</i>			1			1	0.3
porosiform scales		3				3	0.9
poracanthodid, forma <i>bifurcata</i>			1	1		2	0.6
poracanthodid. scales	7	5	3			15	4.7
ischnacanthid tooth whorls F	1		1			2	0.6
acanthodian morph 2 cf. forma <i>bifurcata</i>		2	1	2		5	1.6
acanthodian morph 3	1					1	0.3
indeterminable acanthodian scales	3	3	2		1	9	2.8
indeterminable acanthodian spines F		2		3	1	6	1.9
Total	78	126	34	47	37	322	
% of 322	24.2	39.1	10.6	14.6	11.5		

is low and there is a low (latero)posterior neck. The anterior basal rim may be rounded and the base is very low, with anterior swelling.

The crown of P9182 (Fig. 54; sample SW 15) is symmetric, and the starting points of the antero-median crown rib and of the crown rims are in line. In P9183 (Fig. 55; sample SW 15) the crown rims have somewhat shifted posteriorwards, away from the anterior basal rim. The base is nearly flat.

A scale identified as *N. athleta* from the Pragian-Emsian of Reefton, New Zealand (Macadie, 1998, fig. 2M, about 0.3 mm long) looks very similar to these Ramsåsa E and *N. minima* (-like) scales.

Big trunk scales (Figs. 56-61). *Descriptions* (2) — (New features printed in italics.) Asymmetric scale P9184 (Fig. 56), Ørvg sample, has a moderately inclined (c. 45°), more or less isosceles triangular crown that is contained within the square base. The flat crown surface faces left (Fig. 56a). The right crown rim is straight anteriorly (Fig. 56a); the anterior part of the other rim is bifurcate. There are two lateral rims on the right side (Fig. 56b, posterior view); one joins the crown rim in the posterior crown half and the second is developed as a wider ledge, which begins at the level of the

Table 7. Acanthodian fishes from Ramsåsa E, sample SW 32 (selection). Taxa $\geq 5\%$ in bold.

						Total	% AcT
Fraction	0.106	0.212	0.355	0.425	0.5		
Number of taxa: 13	4	8	7	5	7		
<i>Nostolepis striata</i>	10	37 [T]	13	7	12	79	40.3
forma 'elegans'		5				5	2.6
forma ' <i>Nostolepis minima</i> '	2		3		1	6	3.1
coronate scales & plates		1				1	0.5
stellate plates <i>sensu</i> Gross, 1971		3	1		3	7	3.6
squamae umbellatae, <i>sensu</i> Gross, 1971 F			1	1	3	5	2.6
<i>Gomphonchus sandelensis</i>		2				2	1
<i>Gomphonchus volborthi</i>	17	30	14	10	7	78	39.8
<i>Radioporacanthodes biblicus</i>				1		1	0.5
porosiform scale		1				1	0.5
ischnacanthid tooth whorl F	1					1	0.5
acanthodian morph 2 cf. forma <i>bifurcata</i>		3	2			5	2.6
indeterminable acanthodian scales			3	1	1	5	2.6
Total	30	82	37	20	27	196	
% of 196	15.3	41.8	18.9	10.2	13.8		

basal corner and reaches the square midposterior crown tip. The three midanterior crown riblets do not reach the latitudinal axis of the scale (Fig. 56b). The left anteromedian riblet is parallel to the inner branch of the left crown rim, the other two are parallel to the anterior part of the right crown rim (Fig. 56a). The median riblet is shortest. Crown rims and riblets are in line, except the rightmost riblet, which projects forward. The crown has *one lateral surface* (Fig. 56c) bounded by the lateral crown rim. The right lateral rim begins at the level of the lateral basal corners. On the lateral surface, a short, eccentric, anterolateral rib runs parallel to the lateral rim. The right crown rim curves up, out, in and out again posteriad (Fig. 56a,c). The smooth upper basal area surrounding the crown is narrow anteriorly and widens lateroposteriorly on one side (the left; Fig. 56b). The lateral basal corners bend ventrad (Fig. 56a). The swollen base makes up *c.* one third of total scale height and is thickest medially.

The posterior crown part (with tip broken off) of asymmetric elongate scale P9185 (Fig. 57; Ørving sample, sole specimen) is twisted *c.* 35° to the left. The greater part of the crown is on the right scale half. The steep crown is triangular and has *two lateral surfaces*. The median and lateral surfaces are slightly lower than their boundary rims. Anteriorly the crown surface is twice as wide as posteriorly. If the posterior crown tip is reconstructed, the length of the crown will increase by at least 25%. The left crown rim is sigmoidal, the curves being situated in the anterior and posterior rim parts; the intermediate and longest part of the rim is straight. The left rim begins further anteriorly than the right rim, which is a similar to the left, but is not sigmoid. Two short anteromedian crown ribs run more or less parallel to the right crown rim. The left rib begins at the same level as the left crown rim, and the right rib at the same level as the right crown rim. Between these two ribs, a third diagonal rib can be seen. The right lateral surface also has a short diagonal anteromedian rib. Both diagonal

Table 8. Acanthodian fishes from Ramsåsa E. TFF based on data from Table 15. Predominant taxa in bold.

Taxa	% TFF		% TFF		specimens	specimens
Sample	SW 14	SW 15	SW 32	P 434a	Peyel	Ørvig
<i>Nostolepis striata</i>	5.4	7	5.2	x	55	21
forma ' <i>elegans</i> '	0.3	0.1	0.3			2
forma ' <i>Nostolepis minima</i> '	0.9	2.2	0.3			
squamae proniae		0.1		x	4	
shoulder girdle plate						1
coronate scales & plates		0.2	0.07	x	7	1
stellate plates <i>sensu</i> Gross, 1971	0.5	0.2	0.5		6	
squamae umbellatae <i>sensu</i> Gross, 1971		0.3	0.3			
arched tooth plates					2	
spines F		0.05		x	26+	
<i>N. striata</i> or poracanthodid jaw bones F					10+	1
' <i>Protoplectrodus</i> ' jaw bone type ¹ F						2
<i>Gomphonchus sandelensis</i>	0.4	1	0.1		1	
<i>Gomphonchus volborthi</i>	4.2	3.9	5.1	x	1	
<i>Poracanthodes? lehmani</i>		0.05				
punctatiform cf. <i>Poracanthodes punctatus</i>		0.05		x		
<i>Radioporacanthodes biblicus</i>		0.05	0.07			
poracanthodid, forma <i>bifurcata</i>		0.1				
poracanthodid scales	0.4	1	0.07	x		
ischnacanthid tooth whorls F		0.1	0.07		2	
ischnacanthid spines F				x	29+	
indeterminable acanthodian platelets	0.1	0.3		x	7	2
acanthodian morph 2 cf. forma <i>bifurcata</i>		0.3	0.3			
acanthodian morph 3 ²		0.05				
indeterminable acanthodian spines F	1.1	0.3				

¹ Ørvig's identification.² Vergoossen (2002c, figs. 118-119).

ribs are directed towards the right crown rim. All ribs fade out approximately at the same latitudinal level. There is an unornamented upper basal zone all around the crown. The low, rectangular base is twice as wide as long.

Asymmetric sole specimen P9187 (Fig. 59) is a bit longer than wide. The crown is so little inclined as to be almost horizontal and is contained within the base. The shape of the crown, as indicated by the crown rims, is roughly triangular. One crown rim is shorter than the other and begins further posteriorly. From their beginning, the rims curve laterad and at the level of the lateral basal corners they curve back centrad to form the midposterior tip. The intermediate surface is almost plane, constricted anteriorly and faces to the right (in posterior view, Fig. 59c). *Five forward projected, regularly spaced, short anteromedian riblets curve up from base and run parallel to the longitudinal axis of the crown.* They fade out before the latitudinal axis of the scale. The riblet closest to the shortest crown rim is placed further posteriorly than the other anteromedian riblets and possibly bifurcates anteriorly (Fig. 59b). There is no lateral crown rim in this scale part; a series of oblique neck ribs can be seen (Fig. 59b). The posteriormost neck rib is the steepest, ending at the point where the longer neck rib from further anterior stops.

Most anteriorly, two oblique neck ribs run parallel to half way along the crown's length. All neck ribs rise from the same level quite close to the upper base and end roughly at the same height. On the opposite crown side (Fig. 59c) there is a bifurcating crown rim and a distinct lateral rim. The lower lateral surface bears a short median rib that runs parallel to the lateral crown rim. The unornamented area surrounding the crown is roughly equally wide all around. Lateroposterior neck low. Rhombic base with moderate central swelling.

P9188 (Fig. 60) shares many features with the preceding scale. It has an only slightly more inclined triangular crown with anterior surface facing midanterior. The crown rims bifurcate anteriorly. The shorter crown rim (Fig. 60a, left) begins slightly further posteriorly than the longer (whose anterior part is more curved than in the preceding scale). Six short anteromedian riblets curve up gradually from the same latitudinal level of the upper base except for the rib closest to the short crown rim; this rib begins further posteriorly and is directed more laterally than the others, which run parallel to the longitudinal axis of the scale and are regularly spaced. There are two pairs of lateral crown rims of which the second and steeper has shifted so far posteriad that the rims of their part might be called posterior crown rims. One rim of the anterior lateral pair is damaged (Fig. 60b, c, right side of scale), whereas the other (Fig. 60c, left side) consists of two parts, anterior and posterior, that do not 'fit close.' Low in the lateroposterior neck a row of small openings marks the entries for the radial neck canals.

P9189 (Fig. 61) is more or less intermediate between P9185 and P9188.

P9186 (Fig. 58) is a damaged, asymmetric, much inclined scale (sole specimen) with the *posterior crown* third *strongly constricted by the deep concavity of the slightly sigmoid crown rims*, especially of the left crown rim (Fig. 58a). Five anterior crown riblets of unequal length, left pair (Fig. 58a) parallel to left crown rim. The other three anterior riblets are grouped together in the right scale half and, in comparison, their course has shifted towards the longitudinal axis of the scale. This crown shows a tendency towards an anterior bilobate split up, as recorded in a scale from Ramsåsa D (Vergoossen, 2002c, fig. 91). The lateral crown surfaces are deeper than the central surface; the left surface (Fig. 58a) has two short, parallel, anterior riblets oriented towards the crown top. The lateral anterior riblets begin slightly further forward of the lateral crown rims. The lateral crown rims are not as concave as the left crown rim (Fig. 58a). The greater part of the ventral crown surface is missing, so that the original shape of the crown is unclear; as it is, the crown looks pyramidal. A wide, smooth anterolateral zone separates the crown from the basal rim. Base (in so far as preserved) is low and centrally convex.

New features and additions to existing features — Deep concavity of (sigmoid) crown rim (10); posterior crown strongly constricted (16); one or two lateral crown surfaces (25, 26); distance between anterior riblets (38); more than two forward projected anteromedian riblets (30, 33, 34).

General and taxon-related remarks on some features

Pyramidoid crown (3) — A crown approaching pyramidal shape was figured from Klinta (Vergoossen, 2002b, figs 32, 33, where the similarity of the crown shape to that

on some coronate plates was mentioned) and from Ramsåsa D (Vergoossen, 2002c, fig. 87), with comment on lateral crown surfaces (feature 24). The presence of lateral crown surfaces does not necessarily imply a pyramidoid shape (Gross, 1947, pl. 26, fig. 9; *N. striata*). I now interpret the scales with pyramidoid crowns as a particular form group. Some climatiid prepectoral spines can have pyramidoid shapes (cf. Miles, 1973, text-fig. 4a; *Ptomacanthus anglicus*) and one of the body regions where the scale morph might be placed is near the shoulder girdle (cf. the reconstruction of *P. anglicus* in Miles, 1973, text-fig. 4). Scales of '*Diplacanthoides furcatus*' Brotzen from Scania (Lehman, 1937, pl. 2, figs. 35, 66) may have pyramidoid crowns. The latter scale (*op. cit.*, fig. 66) shows a certain likeness to P9186.

Strong constriction of posterior crown (16) — Produced by deep concave crown rim(s), in combination with sigmoid rims (or not) (10). This feature has never been mentioned in *Nostolepis* or illustrated from *Nostolepis striata* trunk scales, but can sometimes be observed on the crowns of coronate plates ascribed to this species (Gross, 1971, pl. 3, figs. 4, 5, 19). Lehman (1937, fig. 66) showed the feature in a relatively small '*Diplacanthoides furcatus*' scale (0.37×0.37 mm) from Saarema. It was also illustrated in scales of *N. multicosata* from the late Lochkovian? of Ellesmere Island (Vieth, 1980, pl. 4, fig. 3a; text-fig. 16b) and of Pragian to Emsian *N. taimyrica* Valiukevicius (1994, pl. 18, fig. 1).

Lateral crown ledges (22) and *lateral crown surfaces* (24) — Possibly difficult to distinguish on the basis of illustrated examples alone. Do the Lochkovian scales of *Nostolepis striata* from the West Qiling Mountains, China (Wang *et al.*, 1998, pl. 1, figs. A-C) have lateral ledges or surfaces? The crown view of one crown (*op. cit.*, fig. Ca) suggests lateral surfaces and pyramidoid shape, but the side view (Cb) disproves at least the latter impression. The ledge or surface of the specimen in figure A (*op. cit.*) possesses one short anterior riblet. The three scales differ morphologically in several other features from each other; the form in figure A might fit within a series grading to 'modified trunk' scales as described below; the scale morph in fig. C, with its wide, smooth surfaces was not observed in Scanian material, and, unless figure Ca offers a rather distorted view, is probably not *N. striata*.

More than two (30) *forward projected* (33) *anteromedian riblets curving up from base gradually* (31) and *running parallel to the longitudinal axis* (37) — A *Nostolepis striata* scale from the upper Pridoli of Manbrook, U.K. (Vergoossen, 2000, pl. 1, fig. 5) shows this feature, but differs greatly from the Ramsåsa E specimens (Figs. 59, 61 herein) in other aspects. The feature also occurs in 'modified' trunk scales (Fig. 63; see below). Differences in arrangement, spacing, position, height, orientation, density and length of the riblets on the anterior and lateral crown must have produced differences at the hydrodynamic microlevel. Perhaps the overwhelming variety of these features provided adaptive advantages, but it is hardly feasible that such variety should increase the swimming speed. Compare in this respect the far more uniform squamation type of Upper Silurian Baltic *N. gracilis*. As is clear from fused trunk scales and also from tesserae (particularly the multicrowned coronate ones, with (partim) separate crowns), differences in anterior/anteromedian rib features also occur in crowns that lie side by side (cf. Gross, 1971, pl. 2, fig. 15; pl. 3, figs. 5, 13; pl. 5, figs. 5, 10; Wang, 1993, pl. 7,

fig. 5a; Vieth, 1980, pl. 4, fig. 9, *N. applicata*; pl. 7, figs. 10, 17, *Canadalepis linguiformis*), together with differences in other crown features. However, in neighbouring crowns, these differences seem fairly well 'attuned to' each other and never extreme, which does not imply that the morphological contrasts between the crowns have been so levelled as to produce gradual or smooth transitions of form. Compare also the neighbouring scales in the squamation of modern sharks (Reif, 1985); the neighbouring crowns of *N. striata* show much greater morphological contrasts.

'Modified' big trunk scales. Descriptions. (3) — These big scales (> 1 mm) with their characteristic morphology were not recovered from other Scanian samples that I described. These scales are usually strongly ridged. The distinction between crown rims (plus intermediate anterior crown surface), lateral crown rims (plus lateral and ventral crown surfaces) and (short) intermediate crown or neck ribs fades, in favour of more and radial main ridges (plus extra intermediate folds) that converge at the posterior/distal tip and with antieriad (often bifurcate) branching. An erect conical, ridged tubercle (monotubercular 'coronate head' scale or plate) might be one of the final phases of the 'transformation.' As a rule, the crown is contained within the base and the degree of scale 'transformation' may be indicated by how far the crown has shifted centrad. The form grading (mostly assumed from observation on microvertebrate material) has as yet not been fully and serially recorded, or discussed in detail and evaluated for any climatiid, or per sample. Morphs of this scale type are known from *Nostolepis striata*, *N. multicosata* or *N. arctica* (Vieth, 1980). The present material is not suited for such an evaluation, but the scales best demonstrating the 'modification process' are described. About the topography of these scales nothing can be stated with certainty.

P9187 (Fig. 59) is very much an ordinary trunk scale and was described in that section. The crown is contained within base, the crown rims are distinct and on one side (Fig. 59c) it has a lateral rim. Whether there is a lateral rim on the other side (Fig. 59b) is less clear.

P9188 (Fig. 60) is a trunk scale (see that section), but the second pair of lateral ridges has shifted so far posteriad as to virtually form a pair of radial posterior crown rims. This scale resembles a fairly big specimen ($0.85 \times 0.52 \times 0.85$ mm) of '*Diplacanthoides decoratus*' (Lehman, 1937, p. 95, fig. 37). Together with a much smaller specimen of '*D. trilobatus*' ($0.35 \times 0.16 \times 0.38$ mm; *op. cit.*, p. 96; fig. 64 III), these scales are the only examples approaching transitional type illustrated by Lehman.

P9190 (Fig. 62) has an inclined crown with a triangular midanterior surface (Fig. 62b). There is a smooth zone between the crown and the basal edge. The right crown rim (Fig. 62a) trifurcates antieriad; the rim proper is a bit thicker than the branches and hardly restricts the crown surface most anteriorly; it has three diagonal, parallel, laterad branches (Fig. 62b, left; with perhaps a shorter fourth most posteriorly). The other crown rim also has three such branches and one centrad branch, which splits anew further antieriad. The long centrad branch runs parallel to the opposite crown rim, and the intermediate space narrows and deepens antieriad (Fig. 62a). The distal part of the crown is blunt and twisted to the right. The lateroposterior neck is smooth, steep and shows small openings for vascular canals that are unevenly distributed. The rhomboid base is low and convex.

Anteriorly, the low, inclined crown of P9191 (Fig. 63) is still close to the basal rim. Posteriorly, the distance to the basal rim is longer. The crown rims branch anteriorly and there are four, forward projected, anteromedian short crown ribs, parallel to the longitudinal axis and fading out approximately at the level of the branching of the right rim in anterior view (Fig. 63a). Laterad of this rim, several diagonal parallel ridges can be seen (Fig. 63b, left), but it is unclear whether these all represent crown rim branches. On the opposite side (Fig. 63b, right) the crown has two posterolateral rims very close to each other. On the largest lateral surface there is a long, intermediate, median, diagonal and parallel rib that does not seem to reach the crown rim. The posterior part of the crown-neck-base interval is obscured. The rhombic base is convex and deep, with anterior swelling (Fig. 63b).

The crown top of asymmetric P9192 (Fig. 64) is missing. The cross section is at least heptagonal (Fig. 64c) with the sides reflecting the surfaces between the chief crown ribs that converge towards the top; *c.* four surfaces are situated in the lateroposterior crown part. The most posterior side of the heptagon is parallel to the most anterior, which is *c.* a quarter longer. From the cross section it can be inferred that this scale is transitional to what have conventionally been called 'head' scales, but this form might also occur near spines. The posterior crown ribbing or rims are difficult to see. The crown is entirely contained within the base; the upper basal area is larger posterolaterally than anterolaterally. In anterior view (Fig. 64a) it is difficult to distinguish between crown rims and lateral crown rims, and here again the cross sectional and posterior view can help decide; the crown rims form the limits of the anteriormost, straight side in the heptagon. The crown and lateral crown rims are fairly straight. Only the crown rims bifurcate anteriorly. The bifurcating points are high up in the crown and lower down (Fig. 64a,b) at the level where the roughly anteromedian crown rib ends; the two branches flanking this rib are sigmoid (with a rightward tendency in anterior view, Fig. 64a; the whole anterior surface faces right). Base rounded rhombic (Fig. 64b). The anterior crown surface shows a certain likeness to that in Fig. 57a.

The crown of P9193 (Fig. 65) is considerably wider. Although the left anterolateral scale part has broken off, this crown is clearly quite different from the preceding. The crown rims are somewhat thickened; the left crown rim (Fig. 65a) is sinuous and bifurcates anteriorly, with one of the bifurcations branching again further anteriorly. To the left of this crown rim, *c.* six, regularly spaced, diagonally centrad, parallel ribs extend from base level to crown rim. There are four more or less parallel, longitudinal midanterior ribs of unequal length, but how far they extend posteriorly is not clear. Posterior to these ribs, the crown surface is low (Fig. 65b). The other lateral side of the crown is hard to interpret because of damage towards the top. Small openings for vascular canals occur in the posterior neck, roughly in midneck position. Base rhomboid and moderately swollen.

In general outline, the inclined crown of P9194 (Fig. 66) is closer to P9193 than to P9192. The crown is low (as in the other two), well contained within base and positioned in the middle. The margin between crown and upper basal rim is rather wide and the distance to this rim is roughly equal. The crown is strongly ridged. All main rims/ridges meet at the midposterior tip. High 'crown rims' enclose the lower median surface in front of the tip; this surface is subdivided by a blunted, long, median rib branching anteriorly (Fig. 66c). The 'crown rims' also branch anteriorly; the left rim is

highly complex in posterior view. Below the crown tip, on the 'ventral' crown surface, are two short, radial ridges (Fig. 66b). These converge with the tip. A fairly large opening for radial neck canals is seen close to the basal edge (Fig. 66a). The groove leading to the opening indicates that the vessel entered from a position only slightly lower than the basal edge.

In P9195 (Fig. 67) the crown is ridged all round and ridge density has almost reached its maximum; total number (counted at upper basal level or higher in case this level is not reached) *c.* 18. The main ridges reach the crown top. The crown is placed in the middle of the rhomboid base and the longitudinal axis of the scale passes from midanterior base through midanterior crown to midposterior crown top and basal corner. The crown rims (distinguished best in lateral view; Fig. 67b) enclose the lowered median crown surface and bifurcate anteriorly (Fig. 67a). The longer antero-medial crown ribs are slightly projected forwards of crown and curve up from upper base (Fig. 67b). The anteromedial crown has a recession from which the shorter anteromedial ribs ascend (Fig. 67a). The anteriormost lateral crown surface (Fig. 67b) has one very short, and two longer diagonal and subparallel, ribs which ascend from the base. The rib higher on this surface is probably a bifurcation of the crown rim. The posterolateral crown surfaces (Fig. 67c) bear no ribs. The opposite posterolateral crown side (Fig. 67c; left) has more rims/ribs developed. Round to oval openings (*c.* $30 \times 30 \mu\text{m}$, *c.* $25 \times 40 \mu\text{m}$) for vascular canals can be seen all around the neck, with some close to rim/ribs. Further widening of this crown, and with extra ridges added, would produce the shape of a tesserata coronata.

Coronate scale/pinnal plate? (Fig. 68, from Ørvig's slide) — The pentagonal basal platform of P9196 bears a median, low, round, ridged tubercle. The fourteen main radial ridges curve up from the base and almost reach the top. A few ridges bifurcate anteriorly, at about one third of their length below the top. The folds between the ridges are shallowly concave. The tubercle is reminiscent of the ornament on the lingual side of a *Nostolepis striata* or poracanthodid jawbone (Fig. 87b). Basal swelling low and deepest medially.

Coronate? scale (Fig. 69) — Two small thelodont scales (one with a *Thelodus sculptilis* crown, the other with a pitted base, and both serving as dimensional contrasts) are attached to multicrowned scale P9197, which has a rhombic convex base. The ridged, apposed crowns or tubercles are nearly erect with pointed tops and directed posteriorly. Some ridges are spinose (Fig. 69b). Scales similar in morphology were not observed in any of the Scanian faunas previously described by me and must derive from a specific body area. Compare with Gross (1971, pl. 3: *Nostolepis striata*, tesserata coronatae), and the "tuberculated scales" on the ventral side of the body, near the shoulder girdle, of *Climatius reticulatus* Agassiz (Ørvig, 1967, pl. 4, fig. 2); also compare scales of Early Devonian '*Nostolepis*' *robusta* (Gross, 1971, pl. 6, figs 12, 17).

Squamae proniae (Figs. 70, 71) — The orientation (anterior-posterior sides) of the stem-like specimen P9198 (Fig. 70) is hard to establish. The dominating, largest cone (blunted but still pointed) is possibly placed anteromedially on the irregularly round crown. The smaller cones have an irregular arrangement and stand either isolated or

adjoining other cones. Most cones are roughly similar in shape and smooth. The crown does not overhang the concave, steep and fairly high neck (c. one-third of total scale height). Around the cones and in the neck are openings, probably for the vascular supply; some may be artifacts. The conspicuous shallow neck groove (Fig. 70a) may represent a vascular or boring tract and is connected to a tiny opening at its sharpest curve. Shorter and deeper tracts can also be seen in the neck (Fig. 70b). The neck passes into the gradual slope of the base, whose outline is irregularly round. The base is the widest part of this squama and concave on the visceral surface. The specimen is a type 2C variant *sensu* Vergoossen (2002a).

The crown ornament of P9199 (Fig. 71) shows a few peculiarities. There is a smooth sculpture-free strip along the posterior crown edge (cf. Gross, 1971, pl. 1, fig. 7b) and one of the lateral edges shows series of small pustules (the whole posterior margin may have been pustulate originally). Tubercles vary greatly in size, but this is not unusual (cf. Gross, 1971, pl. 1, figs. 10b, 13b). The bulk of the larger tubercles is concentrated on the anterior crown half and suffered less from erosion than the posterior ones. The largest anterior tubercle is situated close to the anteriormost pustules and has crenate or nodose ridges. Many tubercles are contiguous with each other. The low neck has openings for the entry of vascular canals. The shape of the thin basal platform is inverted V-like. This squama pronia is intermediate between form types 1 and 3, and between A and B ornament *sensu* Vergoossen (2002a).

Tooth plate (Fig. 72) — Such terms as anterior, posterior, *etc.*, denote direction in relation to the object. For orientation on the body, terminology (labial, lingual) has been adopted from Miles (1973), who described and figured similar tooth plates from tooth arcades (*in situ*) marginal on the jaw in the climatiid *Ptomacanthus anglicus*.

Arched plate P9200 bears a median row of c. seven separate teeth that increase in size posteriad/linguad. The four anteriormost teeth are small bumps; this condition probably results from lifetime wear. From tooth four posteriad, the teeth are blade-shaped and more or less rectangular in outline, except the last, which is rounded. The edges of the blades are blunted. The last blade has a slightly concave anterior/labial surface, the other blade surfaces are flat. The last two blades lean slightly backwards. The last blade (number seven) is highest, the last but one (number six) widest. Openings for the vascular system can be observed at the transition from posterior blade surface to upper basal platform in blades six and seven. There are also openings lower on the lateroposterior base (Fig. 72a). The base widens posteriad (the blades extend across the entire width of the upper base), and has steep lateral and posterior slopes. Ventrally it is concave. Basal platform; length c. 1.5 mm, width c. 0.73 mm, height c. 0.85 mm. Width of smallest tooth/bump c. 0.13 mm, of widest tooth blade c. 0.61 mm. Highest blade c. 0.4 mm.

Spines — *General remarks.* The large spine fragments, with smooth ribs or noded, are fragile and some got destroyed while being mounted for SE microscopy. Well-preserved, complete spines from Ramsåsa E, prepared by Peyel (see above) are stored at the NRS. Since detailed examination of this material is to be preferred to the study of fragments, I confine myself herein to briefly characterising the best remains. On the whole, the spine fragments from Ramsåsa E agree with the descriptions by Gross

(1971) of *Nostolepis striata* and '*Gomphonchus*' spines from Upper Silurian 'Beyrichienkalk' erratics and from Ohesaare, in both morphology and histology (so far as the latter could be studied).

Nostolepis striata spines (Figs. 73-80) — Since the work by Gross (1947, 1971), Upper Silurian spines from the Baltic area with radial rows of nodes have been assigned to the marine climatiid *N. striata* on the basis of their analogy to the spines of the genus *Climatius* from British Old Red Sandstone (ORS) deposits. Nodose climatiid spines from ORS (or older) deposits in Great Britain and elsewhere were discussed and figured by Ørving (1967), Miles (1973) and Denison (1979). More recently Wang (1993) described and figured prepectoral or intermediate spines assigned to *N. striata* from Lower Devonian faunas from Celtiberia (Spain), associated with *N. gracilis* and several other *Nostolepis* species and shark remains (see also below). Gross (1971, p. 29) saw no way of distinguishing *N. striata* from *N. gracilis* spines ("presuming this has spines"; Burrow, pers. comm.).

Nostolepis gracilis has not been recorded from the Öved Sandstone Formation (ÖSF). Some Scanian *Nostolepis* scales might represent regional variants of *N. striata* cf. Denison (1979, p. 28); also compare with Vergoossen (2003a) on '*Diplacanthoides*' taxa described by Lehman (1937), on scales of the *elegans* and *N. minima*-like form groups and on modified trunk scales. Additional nostolepid or climatiid taxa could be present in some ÖSF faunas (Vergoossen, 2002c, 2003b: acanthodian morphs 3 and 5, respectively). Such observations are complicating factors when one wishes to assign the spines in the conventional manner.

Intact climatiid pectoral spines are easily recognisable, but not present. Other spine types were described as form groups, presumably from different body positions, by Gross (1971). Factual position on the body of the several form groups remains unknown, but is also inferred from the shoulder girdle of British and Podolian climatiids as described by Miles (1973) and Ørving (1967). The group of subrounded to oval, short spines with wide open proximal basal end and radial rows of superficial nodes reaching down from the distal point (e.g., Gross, 1971, pl. 8, figs. 3, 9, 10; pl. 10, figs. 10, 11) must have accommodated prepectoral or intermediate/prepelvic spines.

Another form group (Gross, 1971, pl. 8, figs. 5-8, 19, 21) is more elongate, straight, and more or less symmetric, with nodose superficial ribs converging near the distal point. The proximal basal end is wide open, but this opening can narrow down. The form group of possibly anal spines is narrow, symmetric and has low rather wide ribs branching from a median rib on the leading edge; there is noded or tubercular superficial ornament near the proximal end (Gross, 1971, pl. 8, figs. 11-17). One fragment (Fig. 78) might be part of a dorsal spine (Gross, 1971, pl. 8, figs. 19, 22-24).

Prepectoral or intermediate/prepelvic spines (Fig. 73) — The anterior/ proximal end (part of base and of spine proper) of P9201 is missing. The spine slopes gradually to its highest point, which is reached at two-thirds of its length. In anterior view (Fig. 73b) the spine has a longitudinal, smooth median ridge. Anteriad a few straight, sharp ridges branch from the median ridge, but most of the ornament consists of rows of smooth nodes, either radial rows (posteriad) or rows that branch from the median ridge. When the branching ornament consists of a combination of ridge and nodes (Fig. 73b), the ridge is uppermost and the nodes are lowermost. Posteriad the

noded rows tend to become slightly concave. The median ridge does not reach the anterior spine part; a row of four nodes is situated anteromedially, but is not linked to the median ridge. At least some of the lateral ridges/rows form chevron-like pairs. The biggest nodes are near the spine margins. Some of the marginal nodes may have been ridged tubercles originally. Gross (1971, p. 29) described the nodes as "sculptured tubercles." In the Scanian spine, the idea of eroded, sculptured tubercles is hard to reconcile with the presence of sharp, uneroded ridges. Spines of this form group from Celtiberia (Lochkovian-Pragian; Wang, 1993, p. 132, pl. 13, figs. 7, 8) differ from the Scanian ones by the exclusively radial arrangement of the nodes, fewer radial rows (seven vs about thrice that number) and the absence of ridges. Judging from the composition of the faunas, the Spanish spines might derive from several other taxa.

Other form groups (Figs. 74-80) including anal? (Figs. 74, 76), pectoral and dorsal spine fragments — The largest and widest proximal spine fragment, P9202 (Fig. 74), is moderately convex in cross section (Fig. 74b) and has its smooth, narrow insertion area preserved. *Circa* eight low, flat-topped, smooth, wide main ribs fan out and some bifurcate proximad (Fig. 74a). Gross (1971) did not mention this type of splitting. The ribs look tabular (rounded angles) in cross section (Fig. 74b). The narrow intermediate grooves broaden proximad. Ribs and intermediate grooves have suffered from erosion. The groove between the top rib and one of the flanking ribs (on the left in Fig. 74b) might have nearly closed up during growth (cf. Fig. 76). Gross (1971, text-fig. 14b) illustrated a similar growth phenomenon in an old, high *N. striata* spine with four growth zones and a closed spine cavity. On one side of the longitudinal axis, the spine is shorter and steeper than on the other (Fig. 74b). There is a wide open (*c.* 120°) central cavity.

P9203 (Fig. 75) is broader and more flattened in cross section (Fig. 75b); it lacks an insertion area and has smooth nodes along the anterior edge. On some of six longitudinal main ribs, splitting off can be seen. All the ribs are low and flat, and straight posteriad; anteriorly they broaden and their outline becomes irregular. The ribs are flanked by openings of the vascular system situated in the intermediate grooves. The base of the spine is wide open.

Convex spine P9204 (Fig. 76) has five main ribs, with short, diagonal, posteriad ridges on the proximal flank of at least one rib (Fig. 76b). The ridges occur on the side facing the longitudinal axis of the spine. The ribs are low, flat and broad, rectangular in cross section (Fig. 76a) and broaden anteriorly. In one place the median rib and one of the flanking ribs have grown together, and have one continuous upper surface. The acute-angled central cavity of the spine is narrower and higher than that of the preceding fragments; the cavity has a vertical wall on one side.

Convex and terraced proximal fragment P9205 (Fig. 77) was well-vascularized and has longitudinal grooves in front of openings for vascular vessels in the preserved insertion area, which narrows proximad and is *c.* 1.2 mm long (cf. length of insertion area, *c.* 0.3 mm, in P9202; Fig. 74a). The six ribs with flat tops are noded/partitioned transversely (cf. with ischnacanthid spine, e.g., P9209; Fig. 81). The leading rib is indistinct and the lateralmost rib on each side is the smallest. The spine has a concave (obtuse-angled) and widely open base. Originally this fragment was much longer, but it disintegrated when manipulated with a brush for photography.

Fragment P9206 (Fig. 78) is more laterally compressed and triangular. The ribs are straight, smooth, low and angular (Fig. 78a, b), and flat-topped proximad. The intermediate flat grooves widen proximad and can hold up to three round to oval openings of vascular canals in a cross row. As a rule vascular openings are aligned at regular distances along (or nearly under) the longitudinal ribs. The nodose ornament differs from that on the 'intermediate' spines; it is elongate and drop-like (Fig. 78b) rather than spherical or tubercular. Vascular openings are also grouped closely around (Fig. 78b) or found under (Fig. 78d) the nodes, which occur especially near the trailing edge. At the distal end of this edge, where the central cavity is closed, finer longitudinal ribs can be seen (Fig. 78c, d). At the distal tip, the cross section of the spine is equilateral-triangular.

Distal spine fragment P9207 (Fig. 79) has five, smooth, parallel ribs branching from the median rib on the leading edge. Below the ribs that form part of the trailing edge, diagonal rows of partly fused, elongate, triangular, mostly smooth denticles can be observed; these may look like crowns of 'forma *elegans*' scales (cf. Vergoossen, 2002c, figs. 94-99) with one or two short anteromedian ridges. The denticles also strongly resemble a scale from the web of the posterior dorsal fin in *Ptomacanthus anglicus* (Miles, 1973, text-fig. 1D). Alternatively, they might have covered a shoulder girdle plate (like the ventrolateral plate, plus spine in the climatiid *Errivacanthus*; Ørvig, 1967). These denticles/scale crowns can fuse laterally (mediad), and small openings (vascular) are arranged along their anterior and posterolateral rims. The branching ribs of the spine have flat tops, and are slightly convex and sometimes tabular (squarish) in cross section. The spine cavity is open and acute-angled (Fig. 79c).

P9208 (Fig. 80) is a similar distal fragment, but more worn and with much sediment adhering to it. Near the trailing edge the ribs pass into elongate nodes and there is a diagonal row of four radially ridged tubercles (Fig. 80b).

Body of fish not known. Some spine, tooth whorl, and jaw bone form groups

Figs. 81- 87.

Ischnacanthid spines (Figs. 81-83) — Only two ischnacanthid scales (Table 1b) were associated with the spine fragments described below. Gross (1947, 1971) assigned the ischnacanthid spine fragments from the Upper Silurian of the Baltic region to *Gomphonchus*, to which he had also referred poracanthodid scales. As a rule these spines are slender and nearly straight, with smooth rounded or flattened longitudinal costae or ribs which number between three and c. thirteen. The median rib forming the leading edge can be higher and wider than the other ribs, and separated from them by deeper grooves. The leading rib, and also the lateral pair that flanks it, can bear sort of Spanish-tiled ornament separated by "Querfurchen" (= transverse furrows; Gross, 1971, p. 62; cf. also the "sillons transversaux" on '*Onchus(?) brotzeni*;' Lehman, 1937). In histological illustrations, however, these transverse partitionings do not show as "Querfurchen," but as barriers/boundary walls or "thresholds" (Gross, 1971, text-figs 25A, 27A; there is no distal overlap of the tiled ornament during growth; see also *op. cit.*, p. 64; this ornament needs further study; cf. also P9910-11, below). The tiled ornament is present on the leading rib and at least two of the flanking lateral rib pairs of P9209 (Fig. 81). The 'transverse furrows' are sigmoid or reclining on the leading rib and straighter on

the lateral ribs (Fig. 81c). The recline is directed proximad. All of the eleven ribs have more or less rounded surfaces (Fig. 81e) and the intermediate grooves are also rounded. The most lateral grooves are narrowest, almost slits. Round to oval openings (for short vascular canals leading to the longitudinal canals) are situated very close to the edge of the ribs, and only rarely in the middle of the intermediate grooves (Fig. 81c). The open central cavity is filled with sediment. The rib pair on the trailing edge is not distinguished by larger size or tubercular ornament (cf. Gross, 1971, pl. 8, fig. 30) and shows a trace of a tunnelling micro-organism (Fig. 81d).

Valiukevicius (1992) was the first to describe poracanthodid spines (pectoral, dorsal, pelvic, anal) based on articulated Lochkovian remains from Severnaya Zemlya (*Zemlyacanthus menmeri*). Whether these spines are morphologically or histologically distinct enough to be recognised in disarticulated fragments remains a matter for detailed comparison. Valiukevicius gave no detailed descriptions and did not mention an insertion area or rib ornament; the surface of the ribs seems rounded (*op. cit.*, text-fig. 11). Blom (1999, p. 68) recorded fragments from the Silurian-Devonian of north Greenland with larger lateral costae and apparently without ornament, or a variation with "smaller ridges occurring as striations on the larger anterior ribs;" such material was not observed and might derive from regional taxa.

P9210 (Fig. 82) has five costae. The open, upper central cavity is rounded, equilateral-triangular in cross section (Fig. 82b). The ribs flanking the small lower cavity along the trailing edge are narrow. In cross-section, the biggest median rib is rounder than the lateral ones (width ratio: c. 5:3:2). The ribs seem smooth, but at higher magnification the upper show partitioning by thin, straight, cross lines, which might be microscopic preservational cracks.

The transverse partitioning of ribs is slightly more noticeable in dorsolateral view of specimen P9211 (Fig. 83). This has nine ribs, of which the leading is more prominent and rounded, whereas the lateral ones have flatter tops (Fig. 83b). Rib width ratio c. 5.5:2:2:1:1. The upper and oldest central cavity (isosceles in proximal cross section; Fig. 83b) is separated by a thick wall from the open lower cavity (more or less similar in outline to the upper) in the proximal spine part. Coarse and fine, subparallel, horizontal basal growth layering and vaguer fine lamination around the central cavities can be discerned in this cross-section.

Arched ischmacanthid tooth plate (Fig. 84) — Posteriorly, the thin and eroded arched plate P9212 widens out to twice its anterior width. The median tooth row consists of at least seven, successive, smooth main cusps that are round in cross section and increase in size posteriad. The largest and most complete cusp (no sharp edges preserved) curves posteriad, but is not geniculate ("knickartig gebogen," Gross, 1957, p. 5) in its lower third. The first and the last cusp of the median row are not accompanied by side cusps. The intermediate main cusps are flanked by a row of side cusps (also round in cross section) on the plate margins, but the number of side cusps in each row (six) is higher than the number of intermediate main cusps (five). Some side cusps show traces of vertical ridges. The orientation and inclination of side cusps in the right row (Fig. 84a) is posterolaterad rather than posteriad, in the left side cusp row these features are not clear. All teeth are surrounded by small openings of the vascular system. The basal plate is not thickened along its margins. Among the '*Gomphodus*'

(= '*Gomphonchus*') variations illustrated by Gross (1947, 1957, 1971), the present tooth plate shows affinity to the ones in Gross (1957, pl. 3, figs. 1a-c, 4a, b), but there are clear differences, e.g., apart from the extreme convexity of the 'Beyrichienkalk' plates, their lateral cusps have tiny side buds. Despite variations related to growth stages of a fish and to placement in the jaw, it is reasonable to argue that from the faunistic point of view the '*Gomphodus*' whorls from erratics represent a morphologically heterogeneous group. There is little or no resemblance of P9212 to a tooth from Ramsåsa, whorls from Öfvedskloster/Helvetesgraven (Lehman, 1937, figs 77, 77 bis; Vergoossen, 1999b, figs. 31-34), to a whorl from the Pridolian of West Qinling Mountains, China (Wang Nianzhong *et al.*, 1998, pl. 1, fig. 1), to most whorls from the Silurian-Devonian of Greenland (Blom, 1999, fig. 41), to that from Lower Devonian northern German erratics (Brotzen, 1934, pl. 2, fig. 15), to those from the Lower Devonian of Palencia (Mader, 1986, pls. 3, 6, 14) or Celtiberia, Spain (Wang, 1993, pl. 15, figs. 12, 13), New South Wales (Burrow, 1995, fig. 4), or Reefton, New Zealand (Macadie, 1998, fig. 2H). The Devonian East-Gondwanan and Ibero-American tooth plates will derive from local taxa. Burrow (pers. comm.) remarked, "On most of the tooth whorls that I have, all the transverse cusps are connected, they are not separated and staggered as on P9212, with base bone tissue visible between them."

Whorl length *c.* 1.31 mm, greatest width *c.* 0.85 mm, greatest height *c.* 0.71 mm. Height of second median main tooth *c.* 0.12 mm, height of seventh and last (biggest) *c.* 0.57 mm; diameter of fourth median main tooth *c.* 0.17 × 0.21 mm (= *c.* 0.36 mm²). Diameter of side cusps 1, 3 (left in anterior view) *c.* 0.1 × 0.1 mm, *c.* 0.12 × 0.11 mm (= *c.* 0.13 mm²), respectively. Height of most posterior right side cusp *c.* 0.2 mm.

The most anterior main teeth (the oldest; Ørvig, 1973) point forwards, whereas the posterior main teeth (the youngest) point backwards, which comes down to a shift in orientation of roughly 90° during growth. This shift is accompanied by a posteriad decrease in the curvature of the basal platform, which is more strongly bent in its anterior part (cf. Fig. 84b). The main teeth must have had a considerable growth impetus after the second (anterior and latitudinal) tooth row had formed. The increase in size of the main cusps seems to mark the beginning of the decrease in curvature of the base and of a faster expansion of the basal platform laterad. It is unlikely that such changes should be restricted to an individual tooth plate; they may reflect important phases in the growth of the fish. For a different interpretation of the growth of the tooth plates and the implications involved, see Gross (1957), who postulated that the teeth on these whorls were formed all at once. Thin sections (Gross, 1957, text-fig. 3) show attachment tissue (Sharpey's fibres) between the teeth, which points towards appositional growth and this growth interpretation of both *Gomphonchus* and *Nostolepis* whorls was given later by Gross (1971, pp. 28, 29). Vergoossen (1999b) described a complex whorl, possibly resulting from lateral fusion of several whorls.

Jawbone remains, Nostolepis striata or poracanthoid? (Figs. 85-87) — What was said about the study of spine fragments in relation to complete spines from Ramsåsa E (see above) also applies to jawbones. On the whole, the jawbone fragments agree in many respects with the Upper Silurian *Nostolepis* (*striata*) jawbones from Baltic-derived erratics from northern Germany (Gross, 1957, 1971), with the *Nostolepis* sp. indet. jawbones from "the Upper Silurian (K4)" of Saaremaa (Ørvig, 1967), and from "the Upper

Silurian or Lowermost Devonian Ramsåsa Beds of Scania" (Ørvig, 1973). The latter included NRS specimen P502 figured by Lehman (1937, pl. 8, fig. 79) as "mâchoire couverte de dents," probably from Ramsåsa site F. As regards other climatiid/*Nostolepis* species from which the Ramsåsa E jawbone fragments might derive, the same restrictions apply as in the case of the *N. striata* spines.

Denison (1976) argued that the *N. striata* jaw bones belonged to the ischnacanthid *Gomphonchus hoppei*, which is known in the Baltic region from the mid-Pridoli upwards and absent from the Scanian sites. The teeth on conventional 'Gomphonchus' jawbones are circular in cross-section (Ørvig, 1967, pl. 2, fig. 3; NRS, P596, from the "Ramsåsa Beds"). The Scanian jawbones might also derive from poracanthodids, which are represented by several taxa in the Ramsåsa E samples (Tables 5-8), although they were not recovered from the material in the Peyel glass tube. Slender, high, pointed, longitudinally crested, triangular main teeth as in the jawbones of the articulated Lochkovian poracanthodid species *Zemlyacanthus menneri* (Valiukevicius, 1992, pls. 2, fig. 1; 3, fig. 3; pl. 4, fig. 2) are lacking. Details of the tuberculation on the medial surface of these jawbones were not recorded.

Descriptions — P9213 (Fig. 85) shows an indeterminable, posterior fragment (= from close to the throat), with a single, longitudinal row of tiny, smooth blade-like teeth on the medial edge of the biting surface. The medial side, which is packed with much worn micro-ornament, is gently convex and tapers labiad (Fig. 85a, b). On the labial side the bone was attached to the jaw cartilage, and has longitudinal and latitudinal canals (Fig. 85b); this side is straight and makes an angle of about 90° with the overhanging bottom part of the occlusal surface. In transverse section, the bone is well vascularized on one end (Fig. 85b), on the other it is dense (Fig. 85a). The rounded, subtriangular tooth bladelets have blunted rims. The largest blades measure (height × width) c. 0.07 × 0.12 mm, 0.08 × 0.1 mm, 0.1 × 0.1 mm. A few ridged tubercles passing into the row of blades can be distinguished near the upper right margin (Fig. 85c). A narrow, longitudinal furrow separates the blades from the remainder of the smooth biting surface and fades out halfway.

P9214 (Fig. 86) shows a fragment where the radially ridged tubercles on the biting surface at the edge of the medial side are larger than the smooth and broken, roughly triangular main tooth and its c. five accompanying side cusps on the labial edge (Fig. 86c). The tubercles are eroded at their top; the ridges branch manifold proximad. Tubercles and teeth are separated by a narrow, flat space (not a groove; Fig. 86b). The broadest surface of the side cusps in the tooth row, and of the tubercles on the medial edge and side (Fig. 86a), faces laterad (labiad and linguad); the broadest surface of the blade-like dentition on the medial edge of P9213 (Fig. 85d) faces anteriad and posteriad, a feature also seen in *Nostolepis* whorls (Fig. 72). The jawbone is straight and steep on the labial side and curved on the medial side. Height of main tooth c. 0.33 mm; height ratio main tooth/lateral cusps c. 10:5:5:4:5:5; width main tooth c. 0.83 mm; width ratio main tooth/lateral cusps c. 50:15:10:9:5:4, width first lateral cusp c. 0.25 mm; height ratio main tooth (top missing)/tubercles c. 4:7:6; height largest tubercle c. 0.58 mm; width ratio main tooth/ tubercles 50: 55: 44; width largest tubercle c. 0.91 mm.

Fragment P9215 (Fig. 87) shows the densely tuberculated medial side. The tops of the radially ridged tubercles can be flattened and smoothed, but below the tops the

Table 9. *Nostolepis striata* scales from Ramsåsa E, sample SW 14.

Scale form group	Scale quantities	
<i>Nostolepis striata</i> trunk scales	43	82.7
forma 'elegans'	2	3.8
forma ' <i>Nostolepis minima</i> '	7	13.5
Total	52 = 48.6% AcT	% of 52
	52 = 6.6% TFF	

Table 10. *Nostolepis striata* scales from Ramsåsa E, sample SW 15.

Scale form group	Scale quantities	
<i>Nostolepis striata</i> trunk scales	129	74.6
forma 'elegans'	2	1.2
forma ' <i>Nostolepis minima</i> '	40	23.1
squamae proniae	2	1.2
Total	173 = 53.7% AcT	% of 173
	173 = 9.4% TFF	

Table 11. *Nostolepis striata* scales from Ramsåsa E, sample SW 32.

Scale form group	Scale quantities	
<i>Nostolepis striata</i> trunk scales	76	84.4
forma 'elegans'	5	5.6
forma ' <i>Nostolepis minima</i> '	6	6.7
Total	90 = 45.9% AcT	% of 90
	90 = 5.9% TFF	

radial ridges (which may bifurcate proximad) are still sharp. The parbasal shape of the mostly separate tubercles varies from round to ellipsoid and semi-triangular. Closest to the biting edge of the jawbone, the tubercles seem to be arranged in longitudinally diagonal and parallel rows, and they increase in size, taking on a more a tooth-like, longitudinally triangular shape. The tubercular arrangement suggests that the fragment is from the posterior half of the jawbone (= the part closest to the throat; posterior is to the right in the figures). The large tubercles in the first row below the top are accompanied by lateral 'cusps' or 'nodules' on the side facing the biting edge. Around the largest tubercles round openings occur (for vascular supply; diameter c. 12 μ m). No distinct teeth are preserved on the biting edge, preservation becomes better down the medial side. In cross-section (Fig. 87c) the ventral concavity marks where the bone was fixed to the jaw cartilage. In the interior bone, lamellae (partim parallel) have developed between vascular spaces. The labial surface is straight. The width of the biting surface is c. half that in P9214. Width of largest tubercles varies between c. 0.65 and 0.3 mm; the smallest tubercles are about 0.05 wide. Highest tubercle c. 0.25 mm.

Discussion —The cross sections through P9213 (Fig. 85b) and P9215 (Fig. 87c) may be compared to those of *Nostolepis striata* from the Ohesaare "Schichten" and from a Baltic-derived erratic (Gross, 1971, text-fig. 9A-C), and to the transverse thin section of the jawbone of *Zemlyacanthus menneri* (Valiukevicius, 1992, text-fig. 9D). Compare

them also with the acanthodian dentigerous jawbone fragments from the Lower Devonian Trundle Group, New South Wales (Burrow, 1995, fig. 3A-D). None of these agree in (combined) details of outline, interior bone lamellae, degree of vascularisation and presence/absence/arrangement of ornament on the median side with the Ramsåsa E fragments; one may suspect more than just growth-related factors to be involved in these differences. Ischnacanthid jawbone fragments from the Upper Silurian of Cornwallis Island, Arctic Canada (Burrow *et al.*, 1999) have lateral teeth which are round in parabasal section.

Scales, but no fish body
***Gomphonchus volborthi* (Rohon, 1893)**

Fig. 88.

Remarks — The specimen looks like another characteristic representative matching Lehman's (1937) forms (inclusive of '*Gomphodus irregularis*' Lehman). A continuous anterior crown rim is lacking, between the rounded smooth lobes, smooth folds mark the transition from crown to neck. However, contrary to scales figured from other Scanian sites (Vergoossen, 2002a-c) and from the Ludlow Bone Bed (Vergoossen, 1999c), the anterior crown shows no trace of sharp-edged radial riblets. This and other morphs assigned to *G. volborthi* need to be histologically examined on better-preserved material. Although the range of morphological variation would seem to be limited and the differences only slight, they should be accounted for, preferably on the basis of an assessment of a large sample from one horizon. The present samples are not suited for this sort of research.

Scale frequencies

General remarks — The numbers in the Tables 1-15 (samples SW 14,15, 32) define such categories as abundant (> 50% AgT, TT, AcT or TFF; see abbreviations with Table 1, above), regular finds (25-40%) and rare (< 5%); these categories are representative. The numbers do not represent absolute values and are biased in respect of facies (rocks from NRS collections sampled between 1920-1940), sample weight (=rock weight) and picking (chiefly 'proportionate' selections).

The residues from the pieces of Ramsåsa E rock dissolved by the author are highly biased in favour of small fish remains; any size category over 0.5 mm is lacking. Nevertheless, these findings agree with observations on faunas from other Scanian rock samples that I dissolved (Vergoossen, 2003a, unpublished). The dimensions stated by Lehman (1937, pp. 93-96) for Scanian fish remains are mostly well below 0.6 mm. (In my experience, rock weight or lithology of Baltic-derived Upper Silurian erratics often give no clue about the dimensions of the fish remains contained in them, very coarse-grained sedimentary rocks excepted.) Sedimentological factors may have played a role, but Larsson (1979, p. 23) found no signs of sorting on the tentaculites and considered post-mortem transport negligible. A relationship is conceivable between sedimentary rock type (fine-grained; insoluble mudstone and shaly particles adhering to the scales) and the contained, small-sized microvertebrates. Biological factors could be involved, for instance, small thelodonts; despite the small size bias, some material seems more

completely represented in terms of the whole fish body than other. This particularly applies to the scales of the thelodonts *Thelodus parvidens* and *T. sculptilis*. In the acanthodian material, on the other hand, fossils from certain body regions (e.g., the mouth) are virtually absent. Some acanthodian body regions often had a cover of smaller scales than the rest of the body, e.g., the fin webs and the tail. In some taxa the squamation consisted of small scales and small scales may also have covered young fish. To what extent such factors play a role in the Scanian assemblages cannot be decided from the present study. Extreme examples of incomplete representation in terms of whole fish body are provided by the poracanthodid remains. These are also among the rarest remains in the samples.

Scale frequencies within site E assemblages — Thelodont scales make up more than 80% of the assemblages in the Ramsåsa E samples (Table 15). Thelodont predominance is in line with the findings from other Ramsåsa sites; C, D, south of church, H (which are not so well documented, however; Vergoossen, 2003a), F (Lehman, 1937). This percentage is one of the highest in mixed Ramsåsa microvertebrate assemblages (i.e., with specimens from several, major taxonomic units) established so far; c. 65% was recorded for Ramsåsa C (Vergoossen, 2003b). Lehman's figures for site F come down to c. 76%. The acanthodians make up less than 20% of the assemblages and, with less than 1%, osteostracans form an insignificant component. Major groups not represented are osteichthyans (cf. Helvetesgraven; Vergoossen, 1999b) and heterostracans (cf. Klinta, Vergoossen, 2002b; Ramsåsa F, Lehman, 1937). Birkeniid scales occur in the Peyel and Ørvig residues, but the data from these residues contrast too strongly with those from samples SW 14, 15, 32 (or, indeed, from other Ramsåsa sites studied by the author) to allow any but the most general numerical comparison.

The Ramsåsa E samples are dominated by one thelodont in particular, viz. *Thelodus parvidens*, both in its widest (Tables 12-14) and in its most restricted sense. The latter, the glabrous scales of *T. parvidens s.s.*, make up between 30 and 45% of all the scales, which is only exceeded by the zone fossil *T. sculptilis*, inclusive of forma *T. radiosus*, in SW 15 (Table 3). In the other two samples the zone fossil is represented by at least 10% fewer scales than the glabrous *T. parvidens*. A third important thelodont component of the Ramsåsa E assemblages are the scales of forma *Thelodus radiosus* (Figs. 30, 31). Elsewhere, I made a case for affinity and form grading of the smoother radiosiform variants to the smooth scales of *T. parvidens s.s.* (Vergoossen, 2003b). The position of the radiosiform scales in the faunas is more prominent than suggested by their role in the body zonation scheme of *T. sculptilis* (Märss, 1986, text-fig. 21, fig. 18; text-fig. 22, fig. ?23). They outnumber the scales of forma *T. trilobatus*, which has a rather prominent role in the scheme of *T. parvidens* by Märss (1986, text-fig. 20, from number 18 onwards). Radiosiform scales make up c. 25% of the *Thelodus sculptilis* scale total in samples SW 14 and 32, and over 18% in sample SW 15.

'Conventional' *Thelodus traquairi* scales are rare in the Ramsåsa E assemblages, which agrees with observations on assemblages from other Scanian sites (Vergoossen, 2003a). They are rare in Lehman's (1937) material (but see Table 16).

Although some of the new thelodont morphs (variants 1-3, forma *baltica*) contribute little to the Ramsåsa E assemblages, their share is comparable to that of the poracanthodid taxa. In other Ramsåsa assemblages (e.g., from sample Q607, Fig. 21;

Table 12. Composition of the squamation of the *Theلودus parvidens* fish body *sensu* Märss (1986); sample SW 14. Taxa and data from Table 2.

Scale form group	Scale quantities	
<i>Theلودus parvidens</i> s.s.	311	84.3
head scales	12	3.3
forma <i>Theلودus pugniformis</i>	1	0.3
forma <i>Theلودus bicostatus</i>	2	0.5
forma <i>Theلودus trilobatus</i>		
multicuspid	40	10.8
monocuspid	3	0.8
Total	369 = 53.9% TT = 46.5% TFF	% of 369

Table 13. Composition of squamation of the *Theلودus parvidens* fish body *sensu* Märss (1986); sample SW 15. Taxa and data from Table 3.

Scale form groups	Scale quantities	
<i>Theلودus parvidens</i> s.s.	587	81.5
forma <i>T. costatus</i>	4	0.6
other head scales	19	2.6
forma <i>Theلودus querceus</i>	2	0.3
forma <i>Theلودus bicostatus</i>	15	2.1
forma <i>Theلودus trilobatus</i>		
multicuspid	79	11
monocuspid	6	0.8
forma <i>Theلودus clavaeformis</i>		
Lehman, 1937	1	0.1
Total	713 = 47.4% TT = 38.8% TFF	% of 713

Table 14. Composition of squamation of *Theلودus parvidens* fish body *sensu* Märss (1986); sample SW 32. Taxa and data from Table 4.

Scale form group	Scale quantities	
<i>Theلودus parvidens</i> s. s.	676	85
forma <i>T. costatus</i>	1	0.1
other head scales	11	1.4
forma <i>Theلودus bicostatus</i>	14	1.8
forma <i>Theلودus trilobatus</i>		
multicuspid	91	11.4
monocuspid	2	0.3
forma <i>Theلودus clavaeformis</i>	1	0.1
Total	796 = 59.9% TT = 52.2% TFF	% of 796

Table 15. Composition of assemblages from Ramsåsa E: totals of major taxonomic groups, per sample.

Sample	SW 14		SW 15		SW 32	
osteostracans	1	0.1	13	0.7		
thelodonts	685	86.4	1503	81.8	1329	87.1
acanthodians	107	13.5	322	17.5	196	12.9
Total	793	% total	1838	% total	1525	% total

Table 16. Thelodont scale frequencies in sample from Ramsåsa quarry. Data from Turner (1984).

Ramsåsa F	sample 2	% TT	sample 3	% TT
Taxon	number of scales		number of scales	
<i>T. parvidens s.s.</i>	14	13	24	27.9
<i>T. costatus</i>	6	5.6	6	7
<i>T. trilobatus</i>	30	28	6	7
<i>T. pugniformis</i>	1	0.9	5	5.8
<i>T. sculptilis</i>	39	36.5	25	29
' <i>T. schmidti</i> '	5	4.7	2	2.3
<i>T. traquairi</i>	6	5.6	18	20.9
<i>Lanarkia</i> sp. cf. <i>L. spinosa</i>	2	1.9		
<i>P. ludlowiensis</i>	3	2.8		
<i>G. alatus</i>	1	0.9		
Total	107			86

Vergoossen, 2003a, chapter 6), they seem less unimportant (more precise data not available). Forma *subulata* specimens occur somewhat more commonly (31 scales), as in the site H fauna (Vergoossen, 2002a), but in other Ramsåsa assemblages (sites C, D; Vergoossen, 2002c, 2003b) their portion is as low as that of the other new morphs. Re-examination of the Helvetesgraven residue (Vergoossen, 1999b) did not yield *subulata* scales.

Loganiids, *Katoporodus* and *Thelodus admirabilis* Märss, 1982, scales were not observed in Ramsåsa E assemblages. This tallies in part with previous observations on Ramsåsa assemblages (Vergoossen, 2003a, chapter 6). Both age-related and other factors might be involved (for loganiids, also see below). Age-related factors will concern relatively slight differences within *T. sculptilis* zone age (see below; Vergoossen, 2003a, chapter 6).

The percentages of the acanthodians *Nostolepis striata* and *Gomphonchus volborthi*, are fairly constant (Table 8). *Nostolepis striata* remains form the main acanthodian component of the Ramsåsa E assemblages (as of all Scanian assemblages). In sample SW 32 the percentage of *G. volborthi* scales comes close to that of *N. striata*. *Gomphonchus sandelensis* (Pander, 1856) and the poracanthodids are rare (Table 8). Low frequencies for these taxa are the rule in all Ramsåsa assemblages examined by me (see below; Vergoossen, 2003a, chapter 6). Considering the low acanthodian frequencies in the samples, it is not surprising that 'specialised remains' (= not deriving from the flanks, but from other, restricted body areas) such as tesserae, squamae proniae and umbellatae, teeth and spines, should also be rare; the most common are spine fragments (mostly indeterminable) and tesserae stellatae. Jawbone fragments are altogether lacking in SW samples. The fact that precisely such 'specialised remains' are so well represented in the Peyel and, to a lesser extent, the Ørving residues, indicates that this material must be highly biased. This is confirmed by the observation that fish fossils smaller than 0.5 mm are missing. With the material available, it makes no sense to try and assign the 'specialised remains' from the Peyel and Ørving residues to the taxa from the SW samples on the basis of frequencies. Not until the assemblages from which these fossils were picked are better known can any such attempt be made.

The greatest taxon diversity in the Ramsåsa E assemblages is seen in the 0.212 sieve fraction. Except for the 0.212 fraction of the SW15 sample residue, the fraction smaller than 0.106 weighed most (because the finest sediment made up the largest portion of the residues), but hardly yielded scales and was not further examined. The fractions with the highest number of taxa and % TT or % AcT have been highlighted in Tables 2-7.

Scale frequencies in T. sculptilis age assemblages compared (inter)regionally — On the whole the samples from the Whitcliffian beds on Gotland (Fredholm, 1989) contain much fewer vertebrate remains (scales/kg) than the ÖSF samples.

Recent figures on thelodont frequencies that include *Thelodus parvidens* s.s. are available from faunas of *T. sculptilis* zone age from Ramsåsa site F (Turner, 1984, table 5.3; see Table 16) [1] and, outside Scania, from bone bed assemblages in the U.K. (Turner, 1973, 2000, tables 4, 5), with *Paralogonia ludlowiensis* (Gross, 1967) represented, but without *T. sculptilis* [2]. Older figures for comparison of scale frequencies are available from Ramsåsa site F (Lehman, 1937). These will be dealt with in the study of samples from that site.

[1] In 'hand' samples 2, 3 from Ramsåsa F (weight per sample c. 1 kg; sample 1 was not considered because of evident errors in the scale quantities), *T. parvidens* s.s. was recorded less commonly than *T. sculptilis*, whereas the scales of the scleritome *T. parvidens sensu* Märss, 1986, outnumber those of *T. sculptilis*. Sample 2 has a much higher percentage of *T. trilobatus* and sample 3 of *T. traquairi* scales than have the Ramsåsa E assemblages. Apart from *Goniporus alatus* Gross, 1967 (sample 2), Turner (1984) reported *Katopородus tricavus* Gross, 1967 (one scale, sample 1), from Ramsåsa quarry. I have also observed these two species in Ramsåsa material, but not in assemblages from the sites that I have described (Vergoossen, 2002a, c, 2003b). Cephalaspid remains and rare *Gomphonchus* scales were mentioned by Turner (1984) only from the rich sample 1, producing scales in a size range of 0.5-1.5 mm within a species (sample 2 yielded small thelodont scales and large acanthodian *Nostolepis striata* and 'cf. *Ptychodictyon*' scales; sample 3 had "large scales"). Considering the enormous amounts of scales (running into six figures, pers. obs.) that even small pieces of rock from Ramsåsa quarry can contain, all these percentages and comparisons should be viewed with caution. Turner (1984) did not state where samples 1-3 were taken in Ramsåsa quarry.

[2] Taking into account the absence of the *Thelodus sculptilis*-*T. admirabilis* scale complex from the Upper Silurian U.K. bone bed faunas, the constituent thelodont taxa (or varieties) per fauna, and their frequency ratios (from 50 g of dissolved rock), show no close similarities (no information is available to me on the number of samples from which each fauna was obtained). The percentages for one and the same component in the U.K. faunas may greatly differ per fauna, also from sites with the same name, although in the latter case the percentages are, as a rule, better attuned. For example, the percentages for *T. trilobatus* vary between 0.7 and 53.3, but for Netherpton 1 and 2 they are 3.7 and 5, respectively (Turner, 2000, table 5). The assemblages from Ramsåsa E do not show such big differences. For instance, forma *T. trilobatus* (inclusive of *clavaeformis*) scales make up c. 12% of the total

number of scales attributed to the squamation of the *T. parvidens* fish (Tables 12-14), and vary between 5.7 and 7.1 of thelodont total. Most figures recorded for *T. trilobatus* by Turner (2000, tables 4, 5) and the figures in this paper do not demonstrate any 'proportionate representation' in relation to the place of this scale type within the scheme for *T. parvidens* by Märss (1986, text-fig. 20, from number 18 onwards).

The scale frequencies per assemblage in the Microvertebrate Standard sequence can only be indirectly and roughly inferred from Märss (1986), who gave categories (rare, common, abundant) in the stratigraphical distribution logs. In the case of *T. parvidens* such inference is only possible for *T. parvidens sensu* Märss, 1986 (which houses several former species in a manner that they can no longer be distinguished individually, along with other scales). I have not detected any close similarities with the frequencies recorded for the Tahula Beds, which have served as a correlation point for the Scanian assemblages (see correlation, below; Vergoossen, 2003a).

Both Ramsåsa sites C and H yielded rare *Loganellia cuneata* (Gross, 1967) (see also Vergoossen, 2003a, chapter 6, table 1), which was not observed in site E samples. Outside the Baltic region, *L. cuneata* is absent from faunas (of *T. sculptilis* zone age, but without *T. sculptilis*) of the *T. parvidens* community *sensu* Turner, 1999, from the U.K. (Turner, 1973, 1984, 2000, tables 3-5). The species is, however, very numerous in Baltic-derived erratics of 'the *T. parvidens* (s.s.) zone', also without *T. sculptilis* (Gross, 1967, p. 9), and seems to be more numerous in the lower than in the higher part of the *T. sculptilis* zone in the East Baltic sequence (Märss, 1986). On Gotland, *L. cuneata* is certainly more frequent (% TTF) in some samples from the basal Eke and parts of the Burgsvik Beds (Fredholm, 1989) than in the Ramsåsa samples examined. It would seem that the frequencies of *L. cuneata* decrease from east to west along the southern margin of Laurussia and perhaps also upwards in the succession (at least in some parts of the Baltic platform) in the *T. sculptilis* zone. Similarly, the frequencies of the loganellid *Paralogania ludlowiensis* would seem to increase (Turner, 1973, 1984; Miller & Märss, 1999); in the Scanian assemblages examined, the number of scales is either very low or this taxon is absent (Vergoossen, 2003a, chapter 6, table 1).

Scale frequencies per taxon per fraction; Thelodonts (Tables 2-4) — The majority of *Thelodus bicostatus* Hoppe, 1931, scales are in the 0.212 fraction, and the majority of the multicuspid forma *T. trilobatus* scales are in the 0.106 and 0.212 fractions, which makes them much smaller than 'average size' (c. 0.8 mm; Gross, 1967, p. 19). Apart from the *subulata* scales, the new *Thelodus* morphs (variants 1-3 with glabrous crowns and the *baltica* morph) are not restricted to a particular fraction. Neither are the radiosiform scales, which were picked most commonly from the 0.212. *Thelodus sculptilis* scales decrease rapidly in number up from the 0.106 (SW 15, 32) or from 0.212 fraction (SW 14). Gross (1967), whose *T. sculptilis* material came from Ramsåsa (probably F), stated 0.4-0.7 (length) and 0.3-0.7 (width) as size ranges.

Acanthodians (Tables 5-7) — Most of the *Nostolepis striata* and *Gomphonchus volborthi* scales are from the 0.106 and 0.212 fractions. All the scales but one of forma '*N. minima*' are restricted to the ≤ 0.325 fractions and the majority is from the 0.212. Most poracanthodid scales are from the 0.106 and 0.212 fractions. As is to be expected from

what is known about their size, the number of squamae umbellatae increases with mesh width.

Scale frequencies of morphs per scleritome species or other taxonomic units above morph level — SW 15 has a ratio of two ischnacanthid tooth whorl fragments in 120 ischnacanthid remains, SW 32 has one in 92 (Tables 6, 7). These three fragments are from the ≤ 0.325 fractions. SW 15 has a ratio of one squama pronia in 64 *N. striata* 'trunk' scales (and if other *Nostolepis* formae are included, one in 85.5). SW 14 has none in 43 and SW 32 has none in 76 'trunk' scales (Tables 9-11).

Correlation

Remarks — (Table 17; Vergoossen, 2003a, chapter 6, charts 1, 2.) The composition of the assemblages from Ramsåsa E, samples SW 14, 15, 32 and P434a, fits within the *Thelodus sculptilis* biozone (Upper Ludlow - Lower Pridoli) *sensu* Märss *et al.* (1995) Scanian assemblages with *T. sculptilis*, like those from the Eke/Burgsvik Beds on Gotland, might be somewhat older than those from the East Baltic Microvertebrate Standard succession (Vergoossen, 1999b, 2002a-c), where the first appearance of the microvertebrate zone fossil is preceded by a hiatus (Jeppsson *et al.*, 1994; Jeppsson & Aldridge, 2000, fig. 2).

The Ramsåsa assemblages interpreted as the youngest within the *T. sculptilis* zone and dated as late Ludlow (late Whitcliffian; Vergoossen, 2002a, 2003b) are the site C assemblage, with *T. admirabilis*, and the site H fauna, with *T. sculptilis* as the predominant species. These factors do not play a role in the site E assemblages. The Ramsåsa assemblage interpreted as the oldest, but still late Whitcliffian, that from site D, sample SW 24 (Vergoossen, 2002c), has relicts of the Leintwardinian species *T. carinatus* (Pander, 1856) *sensu* Märss (1986). The new *Thelodus* and acanthodian scale morphs associated with these taxa are shown in Table 17 (data from Vergoossen, 2002a, c, 2003b, unpublished).

As regards the acanthodians, the number of small *Nostolepis minima*-like scales in site E sample SW 15 is especially striking. This morph might be part of the '*elegans*' scale group. Extremely rare, new forma *bifurcata* specimens are only shared with the site C assemblage (Vergoossen, 2003b). From Table 17 it would seem that the Ramsåsa E assemblages tend to side with the younger Ramsåsa assemblages.

The main arguments in favour of a late Whitcliffian age (Vergoossen, 2003a) for the Scanian microvertebrate assemblages examined (with an adjustment for the occurrence of *Katoporodus*, Fig. 92, in the Helvetesgraven faunas) need not be repeated here. Other interpretations can be put forward for some of the age-related interpretations of the data (Vergoossen, 2003a, chapter 6). Within the Baltic region, and allowing for local differences in faunal composition, the Ramsåsa E assemblages fit within the late Whitcliffian Ramsåsa assemblages that were correlated (on the basis of the fish microfossils alone) with (the lower part of) the Estonian Tahula Beds and the lower part of the Standard *Thelodus sculptilis* zone (Vergoossen, 2003a, chapters 4-6). Alternatively, if the interpretation of the invertebrate data from the Öved Sandstone Formation is followed (Vergoossen, 2003a, chapter 6), all the Scanian ÖSF microvertebrate assemblages are of early Pridoli age. The material from the Peyel residue and Ørving slides does not contradict a *T. sculptilis* zone age (late Ludlow-early Pridoli).

Table 17. Distribution of some new Ramsåsa morphs and associated age-related thelodont taxa. Key: + = associated with 'oldest' assemblage; X = associated with 'youngest'.

Ramsåsa site samples	D, SW 24	D, Q685	C	H	E
<i>T. parvidens</i> , var. 1, 3	+	+		+	+
<i>T. parvidens</i> , var. 2	+	+	+	+	+
<i>Thelodus</i> sp. indet., forma <i>baltica</i>		X	X		X
<i>Thelodus</i> sp. indet., forma <i>subulata</i>	+	+	+	+	+
<i>T. admirabilis</i>			X		
<i>T. carinatus</i>	+				
<i>L. cuneata</i>			X	X	
<i>P. ludlowiensis</i>	+		+		
<i>N. striata</i> , forma <i>minima/elegans</i>	e		e	m/e	m/e
indeterminable poracanthodid, forma <i>bifurcata</i>			X		X

Frequencies and correlation with the Tahula Beds — The correlation of the Ramsåsa E assemblages with those of the Tahula Beds enables rough comparison of taxon frequencies. One of the most striking differences is in the frequencies for *Gomphonchus*; in the logs illustrating the vertical stratigraphical distribution of the microvertebrate taxa in the Tahula Beds (Märss, 1986), *Gomphonchus (sandelensis = partim G. volborthi, pers. obs.)* is often represented as an abundant faunal element. These high frequencies are not related, however, to the distribution of the *Gomphonchus* scales over one of the facies belts of the Silurian basin (I-III, lagoonal to open shelf). As regards the lithologies of the samples with high frequencies of *Gomphonchus* from the Tahula Beds, distinct differences in lithological composition between these samples and the ones from Ramsåsa E (with low frequencies) may be observed, for instance, in the log for the Sörve 514 core (Märss, 1986, fig. 39, clayey marls).

Acknowledgements

Ulf Borgen is kindly thanked for loan of NRS material. Bert Boekschoten (Rijksuniversiteit Groningen; RUG), Susan Turner (Queensland Museum) and Carole Burrow (University of Queensland) read the manuscript, and made valuable suggestions to improve it. Jan Zagers (Biology Centre, RUG) made the SEM photos, for which I also thank Ietse Stokroos. Wiebe Haaima and Jim Robot (Graphic Service Centre, RUG) prepared the scan images for publication. Martin Staal and Ger Telkamp (Laboratory for Plant Physiology, Biology Centre, RUG) made available digital camera and microscopic facilities to take the histological photos.

References

- Agassiz, J.L.R. 1839. In Murchison, R.I., *The Silurian System* (1st edition). London: 768 pp.
- Afanassieva, O. B. 1999. The exoskeleton of *Ungelaspis* and *Ateleaspis* (Osteostraci, Agnatha) from the Lower Devonian of Severnaya Zemlya, Russia. *Acta Geologica Polonica*, 49: 119-123.
- Blicek, A. & Janvier, P. 1999. Silurian-Devonian vertebrate dominated communities, with particular reference to agnathans. In Boucot, A.J. & Lawson, J.D. (eds), *Palaeocommunities - A Case Study from the Silurian and Lower Devonian*: 79-105. Cambridge University Press, Cambridge.

- Blicek, A. & Turner, S. 2000. IGCP 328: Palaeozoic Microvertebrates final scientific report-Introduction. *Courier Forschungsinstitut Senckenberg*, **223**: 1-67.
- Blom, H. 1999. Vertebrate remains from Upper Silurian-Lower Devonian beds of Hall Land, north Greenland. *Geology of Greenland Survey Bulletin*, **182**: 1-80.
- Blom, H., Märss, T. & Miller, C.G. 2002. Silurian and earliest Devonian birkeniid anaspids from the Northern Hemisphere. *Transactions of the Royal Society of Edinburgh: Earth Sciences*, **92**: 263-323.
- Blom, H., Märss, T. & Miller, C.G. 2003. A new birkeniid anaspid from the Upper Silurian of Skåne, south Sweden. *Geologiska Föreningens i Stockholm Förhandlingar*, **125**: 57-61.
- Brotzen, F. 1934. Erster Nachweis von Unterdevon in Ostseegebiet durch Konglomeratgeschiebe mit Fischresten. II. Teil (Paläontologie). *Zeitschrift für Geschiebeforschung*, **10**: 1-65.
- Burrow, C. 1995. Acanthodian dental elements from the Lower Devonian Trundle Beds, New South Wales. *Records of the Western Australian Museum*, **17**: 331-341.
- Burrow, C.J., Vergoossen, J.M.J., Turner, S., Uyeno, T.T. & Thorsteinsson, R. 1999. Microvertebrate assemblages from the Upper Silurian of Cornwallis Island, Arctic Canada. *Canadian Journal of Earth Sciences*, **36**: 349-361.
- Denison, R.H. 1976. Note on the dentigerous jaw bones of Acanthodii. *Neues Jahrbuch für Geologie und Paläontologie, Monatshefte*, **1976**: 395-399.
- Denison, R.H. 1979. Acanthodii. In Schultze, H.-P. (ed.), *Handbook of Paleichthyology. Volume 5*: 1-62. G. Fischer Verlag, Stuttgart.
- Dzik, J. 2000. The origin of the mineral skeleton in chordates. *Evolutionary Biology*, **31**: 105-154.
- Fredholm, D. 1988a. Vertebrates in the Ludlovian Hemse Beds of Gotland, Sweden. *Geologiska Föreningens i Stockholm Förhandlingar*, **110**: 157-179.
- Fredholm, D. 1988b. Vertebrate biostratigraphy of the Ludlovian Hemse Beds of Gotland, Sweden. *Geologiska Föreningens i Stockholm Förhandlingar*, **110**: 237-253.
- Fredholm, D. 1989. Silurian vertebrates of Gotland, Sweden. *Lund Publications in Geology*, **76**: 1-47.
- Fredholm, D. 1990. Agnathan vertebrates in the Lower Silurian of Gotland, Sweden. *Geologiska Föreningens i Stockholm Förhandlingar*, **112**: 61-84.
- Grönwall, K.A. 1897. Öfversikt af Skånes yngre öfversiluriska bildningar. *Geologiska Föreningens i Stockholm Förhandlingar*, **19**: 188-244.
- Gross, W. 1947. Die Agnathen und Acanthodier des obersilurische Beyrichienkalks. *Palaeontographica, A*, **96**: 91-158.
- Gross, W. 1957. Mundzähne und Hautzähne der Acanthodier und Arthrodiren. *Palaeontographica, A*, **109**: 1-40.
- Gross, W. 1961. Aufbau des Panzers obersilurischer Heterostraci und Osteostraci Norddeutschlands (Geschiebe) und Oesels. *Acta Zoologica*, **42**: 73-150.
- Gross, W. 1967. Über Thelodontier-Schuppen. *Palaeontographica, A*, **127**: 1-67.
- Gross, W. 1968. Die Agnathen-fauna der silurischen Halla-schichten Gotlands. *Geologiska Föreningens i Stockholm Förhandlingar*, **90**: 369-400.
- Gross, W. 1971. Downtonische und dittonische Acanthodier-Reste des Ostseegebietes. *Palaeontographica, A*, **136**: 1- 82.
- Hoppe, K.H. 1931. Die Coelolepiden und Acanthodier des Obersilurs der Insel Oesel. *Palaeontographica*, **76**: 35-94.
- Janvier, P. 1996. *Early Vertebrates. Oxford Monographs on Geology and Geophysics*, 33. Oxford University Press, Oxford: 392 pp.
- Jeppsson, L. 1974. Aspects of Late Silurian conodonts. *Fossils & Strata*, **6**: 1-54.
- Jeppsson, L. & Aldridge, R.J. 2000. Ludlow (late Silurian) oceanic episodes and events. *Journal of the Geological Society*, **157**: 1137-1148.
- Jeppsson, L. & Laufeld, S. 1986. The late Silurian Öved-Ramsåsa Group in Skåne, south Sweden. *Sveriges Geologiska Undersökning, Series Ca*, **58**: 1-45.
- Jeppsson, L., Viira, V. & Männik, P. 1994. Silurian conodont-based correlations between Gotland (Sweden) and Saaremaa (Estonia). *Geological Magazine*, **131**: 201-218.
- Larsson, K. 1979. Silurian tentaculitids from Gotland and Scania. *Fossils & Strata*, **11**: 180 pp.

- Lehman, J-P. 1937. Les Poissons du Downtonien de la Scanie (Suède). *Mémoire de la Faculté des Sciences de l' Université de Paris, N° d'ordre*, **664**: 1-98.
- Macadie, I. 1998. Lower Devonian fossil fishes from Reefton, New Zealand. *Records of the Canterbury Museum*, **12**: 17-29.
- Mader, H. 1986. Schuppen und Zähne von Acanthodiern und Elasmobranchiern aus dem Unter-Devon Spaniens (Pisces). *Göttinger Arbeiten zur Geologie und Paläontologie*, **28**: 59 pp.
- Märss, T. 1982. *Thelodus admirabilis* n. sp. (Agnatha) from the Upper Silurian of the East Baltic. *Eesti NSV Teaduste Akadeemia Toimetised*, **31. Kõide Geoloogia**, **3**: 112-116.
- Märss, T. 1986. Silurian vertebrates of Estonia and west Latvia. *Fossilia Baltica*, **1**: 1-104. [In Russian, with English abstract.]
- Märss, T. 1999. A new Late Silurian or Early Devonian thelodont from the Boothia Peninsula, Arctic Canada. *Palaeontology*, **42**: 1079-1099.
- Märss, T., Fredholm, D., Taalima, V., Tuner, S., Jeppson, L. & Nowlan, G. 1995. Silurian vertebrate biozonal scheme. *Géobios, Mémoire Spécial*, **19**: 369-372.
- Märss, T. & Karatajute-Talimaa, V. 2002. Ordovician and Lower Silurian thelodonts from Severnaya Zemlya Archipelago (Russia). *Geodiversitas*, **24**: 381- 404.
- Märss, T. & Miller, C.G. 2002. Thelodonts and associated conodonts from the Llandovery lowermost Lochkovian of the Welsh Borderland. In: Satkunas, J. & Lazauskiene, J.(eds), *Extended Abstracts, Fifth Baltic Stratigraphic Conference, Basin Stratigraphy - Modern Methods and Problems, September 22-27, Vilnius*: 120-121. Geological Survey of Lithuania, Vilnius.
- Miles, R.S. 1973. Articulated acanthodian fishes from the Old Red Sandstone of England, with a review of the structure and evolution of the acanthodian shoulder-girdle. *Bulletin of the British Museum (Natural History)*, Geology, **24**: 113-213.
- Miller, C.G. & Märss, T. 1999. A conodont, thelodont and acanthodian fauna from the Lower Pridoli (Silurian) of the Much Wenlock Area, Shropshire. *Palaeontology*, **42**: 691-714.
- Ørvig, T. 1967. Some new acanthodian material from the Lower Devonian of Europe. *Zoological Journal of the Linnean Society of London*, **47**: 131-153.
- Ørvig, T. 1973 Acanthodian dentition and its bearing on the relationships of the group. *Palaeontographica, A*, **143**: 119-150.
- Pander, C.H. 1856. *Monographie der fossilen Fische des Silurischen Systems der Russisch Baltischen Gouvernements*. St. Petersburg: 91 pp.
- Reif, W.-E. 1985. Squamation and ecology of sharks. *Courier Forschungsinstitut Senckenberg*, **78**: 1-255.
- Ritchie, A. 1967. *Ateleaspis tessellata* Traquair, a non-cornuate cephalospid from the Upper Silurian of Scotland. *Zoological Journal of the Linnean Society of London*, **47**: 69-81.
- Rohon, V. 1893. Die obersilurischen Fische von Oesel. II. Theil. *Mémoires Académie Impériale des Sciences de St. Pétersbourg*, **41** (5): 1-124.
- Spjeldnaes, N. 1950. On some vertebrate fossils from Gotland, with some comments on the stratigraphy. *Arkiv för Mineralogi och Geologi*, **1**: 211-218.
- Turner, S. 1973. Siluro-Devonian thelodonts from the Welsh Borderland. *Journal of the Geological Society of London*, **129**: 557-584.
- Turner, S. 1984. *Studies on Palaeozoic Thelodonti (Craniata: Agnatha)*. Unpublished Ph.D. thesis, University of Newcastle-upon-Tyne.
- Turner, S. 1999. Early Silurian to Early Devonian thelodont communities. In: Boucot, A.J. & Lawson, J.D. (eds), *Palaeocommunities - A Case Study from the Silurian and Lower Devonian*: 42-78. Cambridge University Press, Cambridge.
- Turner, S. 2000. New Llandovery to early Pridoli microvertebrates including Lower Silurian zone fossil, *Loganellia avonia* nov. sp., from Britain. *Courier Forschungsinstitut Senckenberg*, **223**: 91-127.
- Valiukevicius, J. 1992. First articulated *Poracanthodes* from the Lower Devonian of Severnaya Zemlya. In: Mark-Kurik, E. (ed.), *Fossil Fishes as Living Animals. Academia*, **1**: 193-213. Acad. Sci., Tallinn.
- Valiukevicius, J. 1994. Acanthodians and their stratigraphic significance. In: *Stratigraphy and Fauna of the Lower Devonian of Tareya Key Section (Taimyr)*: 137-197, 236-243. Nedra, Leningrad. [In Russian.]
- Valiukevicius, J. 1998. Acanthodians and zonal stratigraphy of Lower and Middle Devonian in East Baltic and Byelorussia. *Palaeontographica, A*, **248**: 1-53.

- Valiukevicius, J. 2000. Acanthodian biostratigraphy and interregional correlations of the Devonian of the Baltic States, Belarus, Ukraine and Russia. *Courier Forschungsinstitut Senckenberg*, **223**: 271-289.
- Vergoossen J.M.J. 1999a. Late Silurian fish microfossils in an East Baltic-derived erratic from Oosterhaule, with a description of new acanthodian taxa. *Geologie & Mijnbouw*, **78**: 231-251.
- Vergoossen, J.M.J. 1999b. Late Silurian fish microfossils from Helvetesgraven, Skåne southern Sweden. (1). *Geologie & Mijnbouw*, **78**: 267-280.
- Vergoossen, J.M.J. 1999c. Siluro-Devonian microfossils of Acanthodii and Chondrichthyes (Pisces) from the Welsh Borderland/south Wales. *Modern Geology*, **24**: 23-90.
- Vergoossen, J.M.J. 2000. Acanthodian and chondrichthyan microremains in the Siluro-Devonian of the Welsh Borderland, Great Britain, and their biostratigraphical potential. *Courier Forschungsinstitut Senckenberg*, **223**: 175-199.
- Vergoossen, J.M.J. 2002a. Late Silurian fish microfossils from Ramsåsa, locality H, Scania, south Sweden, with some remarks on the body zonation scheme used in thelodont studies. *Scripta Geologica*, **123**: 41-69.
- Vergoossen, J.M.J. 2002b. Late Silurian fish microfossils from Klinta and Rinnebäck's Bro (Scania, south Sweden), with remarks on the morphology of *Nostolepis striata* trunk scales. *Scripta Geologica*, **123**: 71-92.
- Vergoossen, J.M.J. 2002c. Late Silurian fish microfossils from Ramsåsa (sites D and 'south of church'), Skåne, south Sweden. *Scripta Geologica*, **123**: 93-158.
- Vergoossen, J.M.J. 2003a. *Fish Fossils from the Upper Silurian Öved Sandstone Formation, Skåne, southern Sweden*. Unpublished Ph.D. thesis, University of Groningen. [www.ub.rug.nl/eldoc/dis/science/ (search with Google).]
- Vergoossen, J.M.J. 2003b. First record of fish microfossils from Ramsåsa, site C, Skåne, southern Sweden. *Scripta Geologica*, **126**: 1-78.
- Vieth, J. 1980. Thelodontier-, Acanthodier- und Elasmobranchier-Schuppen aus dem Unter-Devon der Kanadischen Arktis (Agnatha, Pisces). *Göttinger Arbeiten zur Geologie und Paläontologie*, **23**: 69 pp.
- Wang Nianzhong, Wang Junqing, Zhang Guorui & Wang Shitao. 1998. The first discovery of Silurian and Early Devonian Acanthodians from Zoige and Tewa counties, West Qiling Mountains. *Vertebrata Palasiatica*, **36**: 268-281.
- Wang, R. 1993. Taxonomie, Palökologie und Biostratigraphie der Mikroichthyolithen aus dem Unterdevon Keltiberiens, Spanien. *Courier Forschungsinstitut Senckenberg*, **161**: 1-205.

Appendix

Nostolepis striata, check list of trunk scale characters.

Crown, general features: 1-8 (symmetry 1-2; shape 3; dimensions 4; plane 5-6; dorsal /ventral surfaces 7-8).

1 symmetric - asymmetric **2** asymmetric: surface facing left - or right **3** shape: triangular (trapezoid) - ellipsoid - pyramidoid - [TES: inverted V-shaped ornament - approximately tubercular] **4** dimensions: narrow - wide (in relation to width of base) - short - long (in relation to length of base) **5** plane: inclined - horizontal **6** inclination: low - moderate - steep **7** dorsal surface: concave - flat **8** ventral surface: midposterior keel

Crown rims 9-15

9 starting position: same latitudinal level - one rim begins further posteriorly **10** anteroposterior path in anterior view: straight - convex - concave - sigmoidal - mixed **11** if mixed, how and in which rim: e.g., centrad twist of the right rim in its upper part **12** anteroposterior path in lateral view: one or both crown rims arched - or not **13** if arched, which rim and where: in its lowermost part - halfway - elsewhere (specify) **14** the angles at which the rims meet posteriorly **15** constricting anterior crown by bending inwards - or not **16** strongly constricting posterior crown

Lateral crown rims 17-22

17 number: left - right **18** starting position of most anterior lateral crown rims: at the level of the lateral corners of the base - further anterior/posterior **19** anteroposterior path in anterior view: straight - curved (convex - concave) **20** bending inwards anteriorly - or not **21** converging with posterior crown tip - ending well below tip **22** narrow (ridge-like) - broad (ledge-like) **23** plain - ornamented

Lateral crown surfaces 24-26

24 present - absent **25** how many: one - two **26** if one, where? on the left - on the right

Anterior crown margin 27-29

27 straight - irregular - with 'Vorkrönchen' or 'Nebenkrönchen'- lobed **28** TES: lobed - separated lobes (in combination with inverted V-shaped crown ornament, feature 3) **29** TES: with median 'bay' present - absent

Anterior riblets (30-38) or lobes (30, 33)

30 present: specify number - absent **31** arched - or ascending from the neck at right angles **32** all sharp-edged - or not (specify) **33** starting position: projected forward of crown rims - at same latitudinal level as crown rim(s) - or posterior to this level **34** starting position: all at the same latitudinal level - varied starting positions (specify) **35** length: of same length - of different lengths - laterad longer - otherwise (specify) **36** orientation: towards lateral left - towards lateral right - longitudinal - mixed (specify) **37** orientation: all parallel (to what?) - partly parallel (to what?) **38** intermediate distance: regular - irregular (specify)

Forward projected anteromedian median rib pair (39-40) or lobe (41)

39 forward projected median pair: present - absent **40** forward projected median pair: of parallel - posteriorly diverging - posteriorly converging riblets **41** forward projecting anteromedian lobe: lobe widens posteriad - lobe narrows posteriad

Median dorsal crown 42-43

42 median opening in lower crown half **43** midposterior ridge

Lateral riblets 44-45

44 present: between lateral rim and crown rim - between lateral rims - on one lateral surface - on both lateral surfaces - left - right; - absent **45** orientation - length - number

Crown in relation to base 46-51

46 crown filling: entire upper basal platform - part of platform **47** unornamented zone of basal platform: anterior - anterolateral - lateral - posterolateral - posterior - all around **48** distance between crown and edge or rim of basal platform (further specified in relation to 47): narrow - wide **49** surface between crown and basal edge or rim of basal platform (not the neck; further specified in relation to 47): concave - flat - sloping **50** crown protruding over base - or not **51** protrusion of crown: posterior tip- posterior/ lateroposterior third - posterior/ lateroposterior half

Neck 52-54

52 lateral - posterior - lateroposterior **53** low - high - moderately high **54** openings of vascular system: none - tiny - medium - large (size relative to 0.1 mm bar)

Neck ribs 55-62

55 developed as: sharp ridges - ribbons (=broader) - sheets (= still broader) **56** straight - curved **57** where: on the left - on the right - posterior - on the left and right - on the left, right and posterior **58** number **59** starting point: near base level - higher in the neck - near the end point of a more anterior neck rib **60** length: as long as the lateral neck - shorter - mixed (specify further) **61** direction: oblique - vertical - in continuation of a more anterior neck rib - parallel to the crown rim - parallel to the lateral crown rim(s) - parallel to other neck rib **62** converging: with posterior crown point - with posterior part of crown rim - with the median part of the crown rim - with the anterior part of the crown rim - with lateral crown rim (low-halfway-high) - with another neck rib

Neck/base junction 63-64

63 with sharp edge - blunted edge - with raised sharp rim (as in some thelodont scales) **64** anterior basal edge or rim: straight - infolding - rounded - angular

Base 65-67

65 shape: rhombic - otherwise (specify) **66** plane: concave - flat - convex (low - deep - moderately deep) **67** dimensions: longer than wide - wider than long.

All material from Ramsåsa site E, unless stated otherwise.
Morphology is shown in Figs 1-88, histology in Figs 89-94.

Plate 1 (Figs 1-11)

Figs 1-10. Osteostracan fishes from the Peyel sample.

- Fig. 1. P 9142. Shield fragment. (a). External view. (b) Detail of external apertures. (c) Lateral view of part of upper margin in 1a.
- Fig. 2. P9037. Shield fragment. (a) External view. (b) Viscerad extension of external ridges seen at the margin of the fragment. (c) Idem. (d) Detail of large marginal ridges with ultrasculpture.
- Fig. 3. P9041. Shield fragment. (a) Longitudinal view. (b) Lateral view.
- Fig. 4. P9050. Shield fragment. (a) External view. (b) Longitudinal view. (c) Detail of 4b, with ridge, interridge connections and ultrasculpture.
- Fig. 5. P9051. Shield fragment. External view.
- Fig. 6. P9057. Scale. (a) Lateral view. (b) Longitudinal view.
- Fig. 7. P9058. Shield fragment. Cross-laminated bone of basal layer.
- Fig. 8. P9059. Shield fragment. (a) External ornament in lateral view. (b) Close up near demarcation groove. (c) Ridges in longitudinal view.
- Fig. 9. P9062. Shield fragment. (a) External view. (b) Longitudinal view.
- Fig. 10. P9106. Shield fragment.

Fig. 11. Anaspid (birkeniid) fishes.

- Fig. 11. P9111. *Ramsåsalepis* Blom *et al.*, 2003. Scale. Peyel sample. (a) Longitudinal view. (b) Detail of ridges.

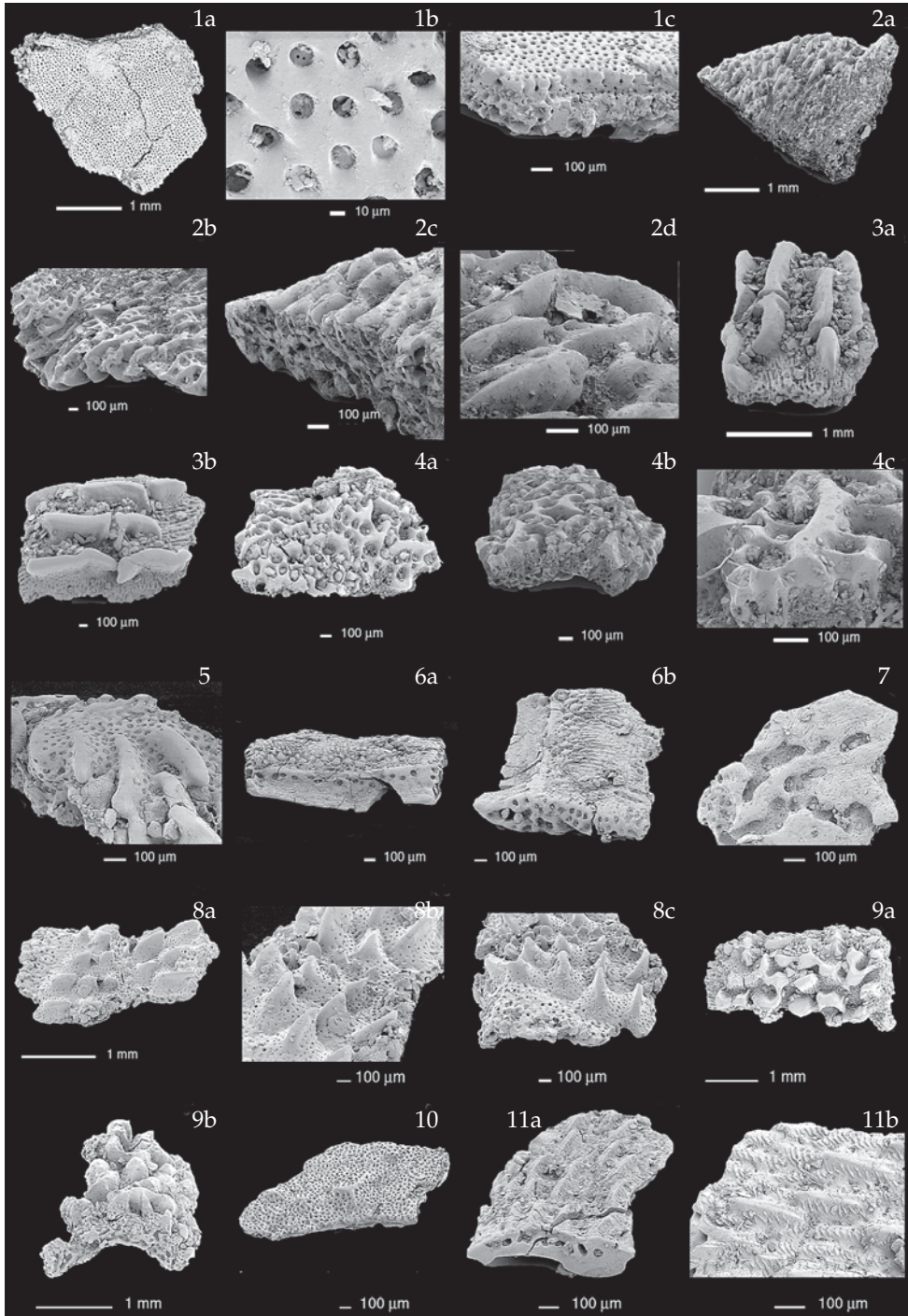


Plate 2 (Figs 12-24)

Fig. 12. Anaspid (birkeniid) fishes.

- Fig. 12. P9125. *Livilepis curvata* Blom *et al.*, 2002. Scale. Ørvig sample. Crown view. (a) From anterior. (b) From posterior.

Figs 13-53. Thelodont fishes. Sample SW 32, unless stated otherwise.

Figs 13-21. Scleritome of *Thelodus parvidens*.

Figs 13-15. Forma *Thelodus parvidens* Agassiz, 1839 *s.s.*, *sensu* Vergoossen 2002c.

- Fig. 13. P9136. Lateral view.

- Fig. 14. RGM 323079. Posterior view. From a Pridolian erratic from the northern Netherlands

- Fig. 15. P9143. Posterior view.

Figs 16-17, 21. Other (cephalopectoral?) forms.

- Fig. 16. P9144. Tricuspid glabrous. (a) Anterior view. (b) Posterior view.

- Fig. 17. P9145. Rhizoid. (a) Crown view. (b) Lateral view.

Figs 18-20. Forma *Thelodus trilobatus* Hoppe, 1931, *sensu* Gross, 1967; included in *Thelodus parvidens sensu* Märss, 1986.

- Fig. 18. P9146. (a) Anterolateral view. (b) Posterolateral view.

- Fig. 19. P9147. (a) Lateral view. (b) Crown view from posterior.

- Fig. 20. P9148. (a) Anterior view. (b) Lateral view. (c) Crown view from posterior.

- Fig. 21. P9149. Calcarate glabrous. (a) Crown view. (b) Lateral view. Ramsåsa. Sample Q607.

Figs 22-24. Scleritome of *Thelodus sculptilis* Gross, 1967. Oral forms.

- Fig. 22. P9150. (a) Crown view. (b) Lateral view.

- Fig. 23. P9151. (a) Crown view. (b) Anterolateral view.

- Fig. 24. P9152. (a) Crown view. (b) Anterior view.

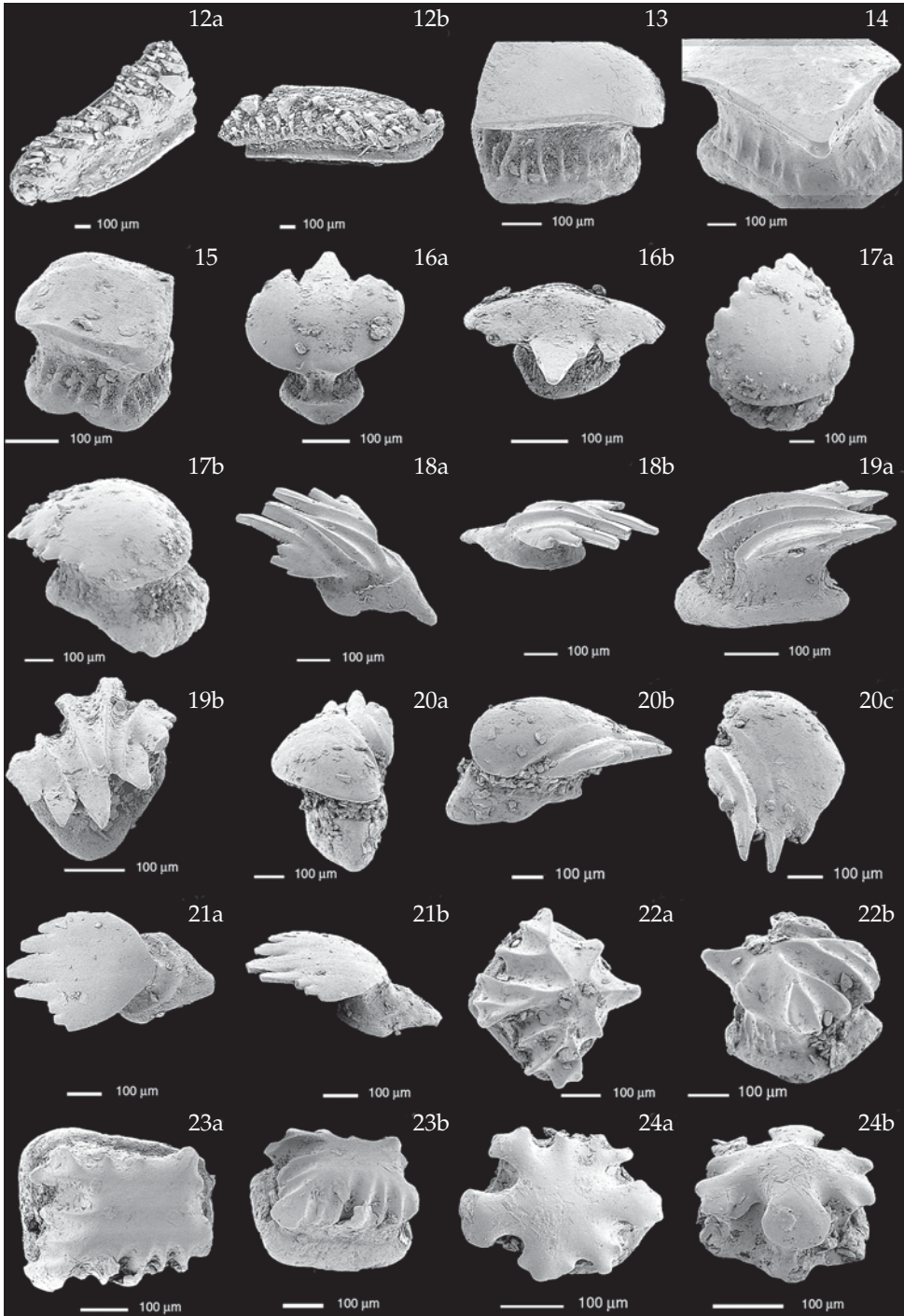


Plate 3 (Figs 25-39)

Figs 25-27; 28-31? 32-34. Scleritome of *Thelodus sculptilis sensu* Märss, 1986.
 Figs 25-27; 28-29?; 32-34. *Thelodus sculptilis* Gross, 1967.

Fig. 25. P9153. Oral? scale. Lateral view. Peyel sample.

Figs 26-31. Cephalopectoral forms.

Figs 30-31. Forma *T. radiosus sensu* Vergoossen, 2003b.

Fig. 26. P9154. Crown view.

Fig. 27. P9155. Crown view.

Fig. 28. P9156. Calcarate glabrous. (a) Anterior view. (b) Lateral view.

Fig. 29. P9157. (a) Anterior view. (b) Lateral view.

Fig. 30. P9158. Crown view.

Fig. 31. P9159. (a) Crown view. (b) Lateral view.

Fig. 32. P9160. Postpectoral scale. (a) Anterolateral view. (b) Posterior view.

Figs 33-34. Basal shape.

Fig. 33. P9161. From visceral.

Fig. 34. P9162. (a) Lateral view of base. (b) From visceral.

Figs 35 - 39. Scleritome of *Thelodus traquairi*?

Figs 35-36. *T. traquairi* Gross, 1967 and Figs 37-39 *Thelodus* sp. indet., subulate form.

Fig. 35. P9163. Conventional form. (a) Lateral view. (b) Basal view.

Fig. 36. P9164. Ramosiform *sensu* Vergoossen, 2003b. (a) Crown view. (b) Lateral view.

Fig. 37. P9165. Subulate form. (a) Anterior view. (b) Lateral view.

Fig. 38. P9166. Subulate form. (a) Anterior view. (b) Detail of ultrasculpture in posterior lateroventral crown.

Fig. 39. P9167. Subulate form. Anterior view.

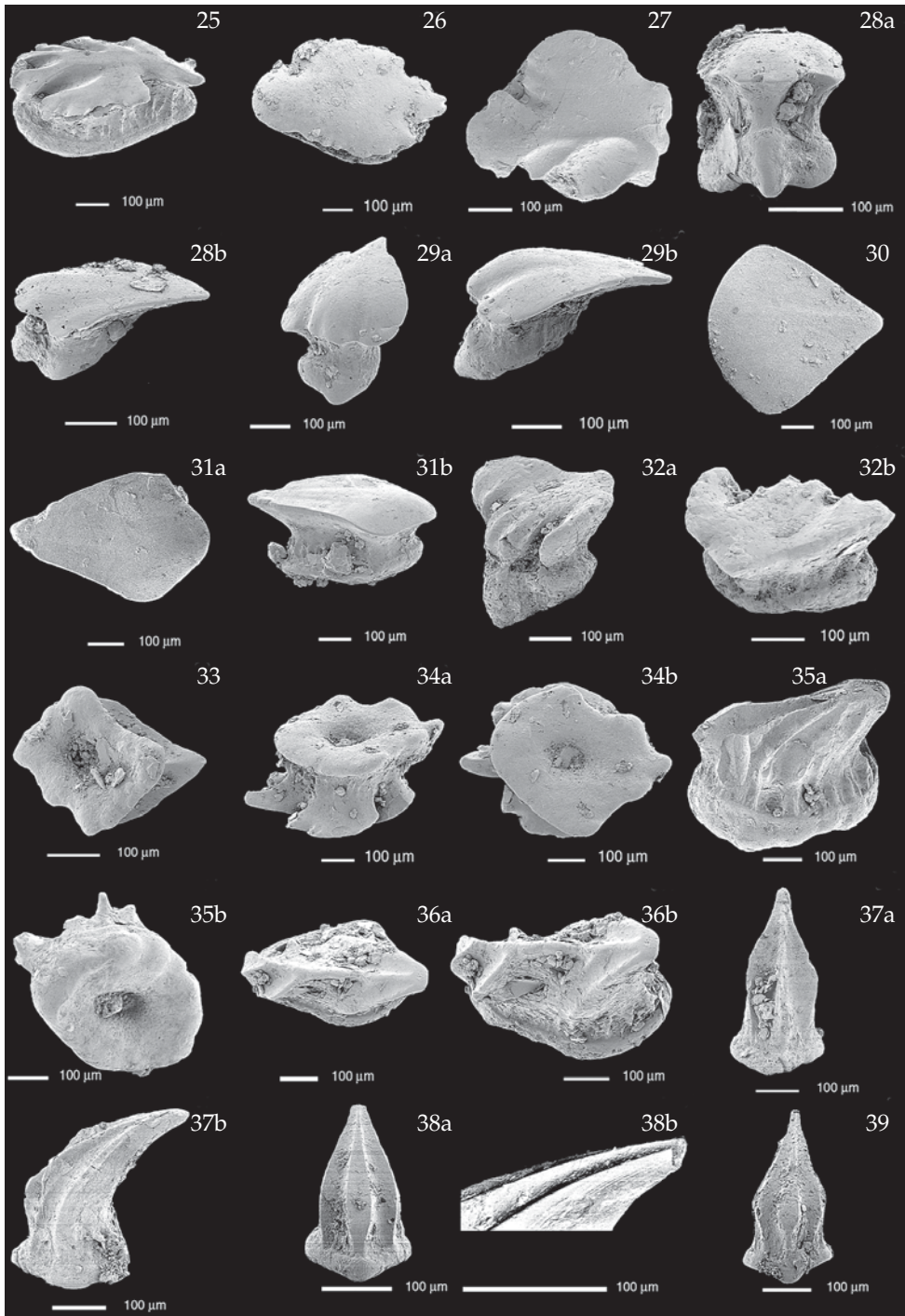


Plate 4 (Figs 40-49)

Figs 40?- 41. Scleritome of *Thelodus traquairi*?

Figs 40?- 41. *Thelodus traquairi* Gross, 1967.

Fig. 40. P9168. (a) Anterior view. (b) Lateral view. (c) Posterior view.

Fig. 41. P9169. (a) Anterior view. (b) Lateral view. (c) Posterior view.

Figs 42-49. *Thelodus* sp. indet., diverse forms.

Fig. 42. P9170. *baltica* form. (a) Anterior view. (b) Lateral view.

Fig. 43. P9171. Postpectoral? scale. (a) Anterior view. (b) Lateral view. (c) Posterior view.

Fig. 44. P9172. Oral? scale. (a) Crown view. (b) Lateral view.

Figs 45-49. Cephalopectoral scales.

Fig. 45. P9173. *bifrontis* form, new form. (a) Crown view. (b) Lateral view.

Fig. 46. P9174. (a) Crown view. (b) Lateral view.

Fig. 47. P9175. (a) Anterior view. (b) Crown view. (c) Detail of anterior crown rim.

Fig. 48. P9176. (a) Crown view. (b) Lateral view.

Fig. 49. P9177. (a) Crown view from posterior. (b) Anterolateral view.

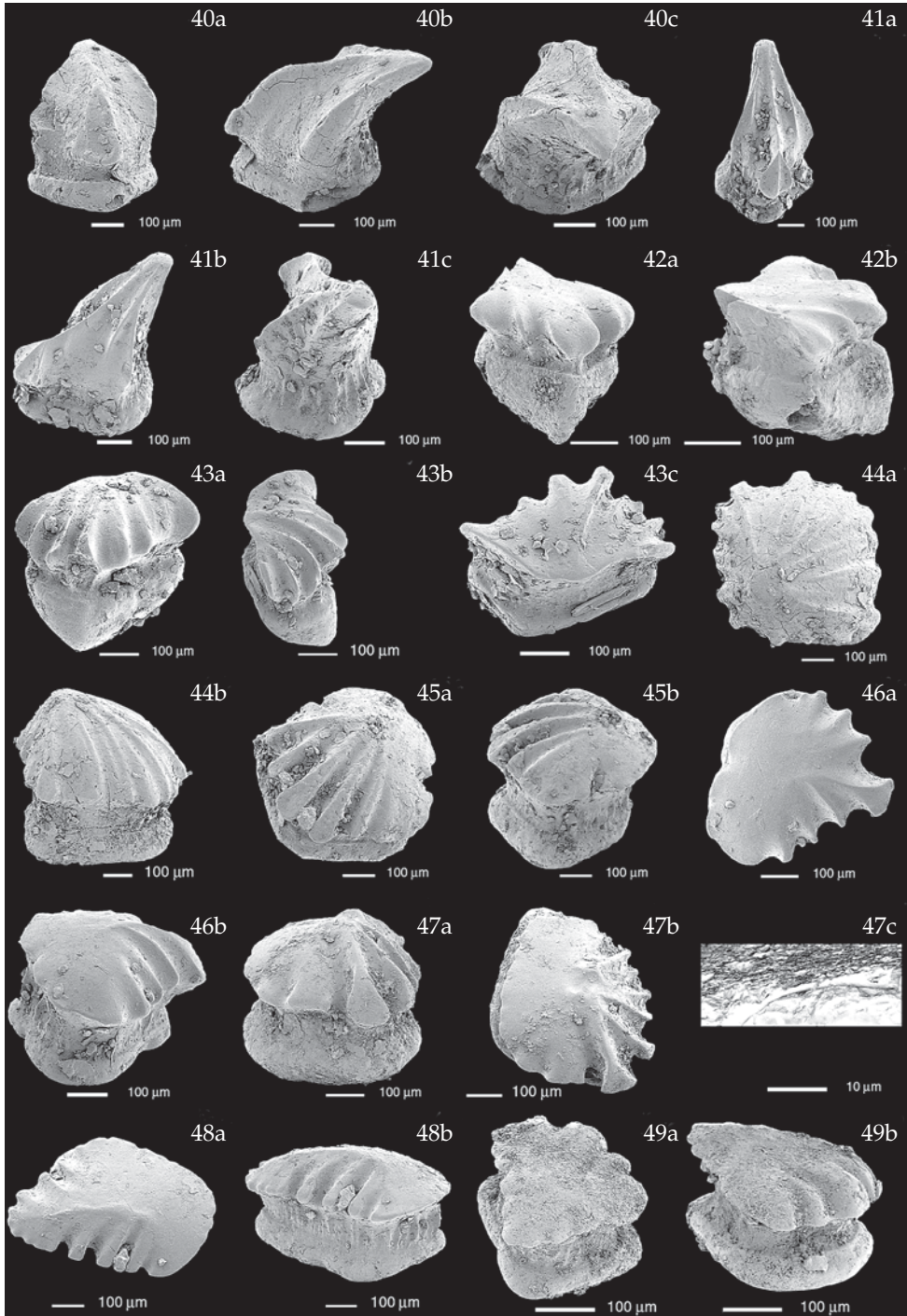


Plate 5 (Figs 50-61)

Figs 50-52. *Thelodus* sp. indet., diverse forms.

Fig. 50. P9178. (a) Crown view from anterior. (b) Lateral view. Sample SW 15.

Figs 51-52. Pinnal? scales.

Fig. 51. P9179. (a) Anterior view. (b) Lateral view.

Fig. 52. P9180. (a) Lateral view. (b) Detail of ultra sculpture in posterior, lateroventral crown.

Fig. 53. Indeterminable, cruciform thelodont scale. P9181. (a) Crown view. (b) More lateral view.

Figs 54-88. Acanthodian fishes, Peyel sample, unless stated otherwise.

Figs 54-61. Scleritome of *Nostolepis striata*. *Nostolepis striata* Pander, 1856 *sensu* Gross 1947, 1971.

Figs 54-55. Morph 'cf. *N. minima*.' Sample SW 15.

Fig. 54. P9182. Crown view.

Fig. 55. P9183. Crown view, from lateral.

Figs 56-61. Big trunk scales.

Fig. 56. P9184. (a) Anterior view. (b) Crown view. (c) Lateral view. Ørvig sample.

Fig. 57. P9185. Anterior view. Ørvig sample.

Fig. 58. P9186. (a) Anterior view. (b) Posterior view.

Fig. 59. P9187. (a) Crown view. (b) Lateral view. (c) Posterolateral view.

Fig. 60. P9188. (a) Anterior view. (b) Lateral view. (c) Posterior view.

Fig. 61. P9189. (a) Posterior view. (b) Lateral view.

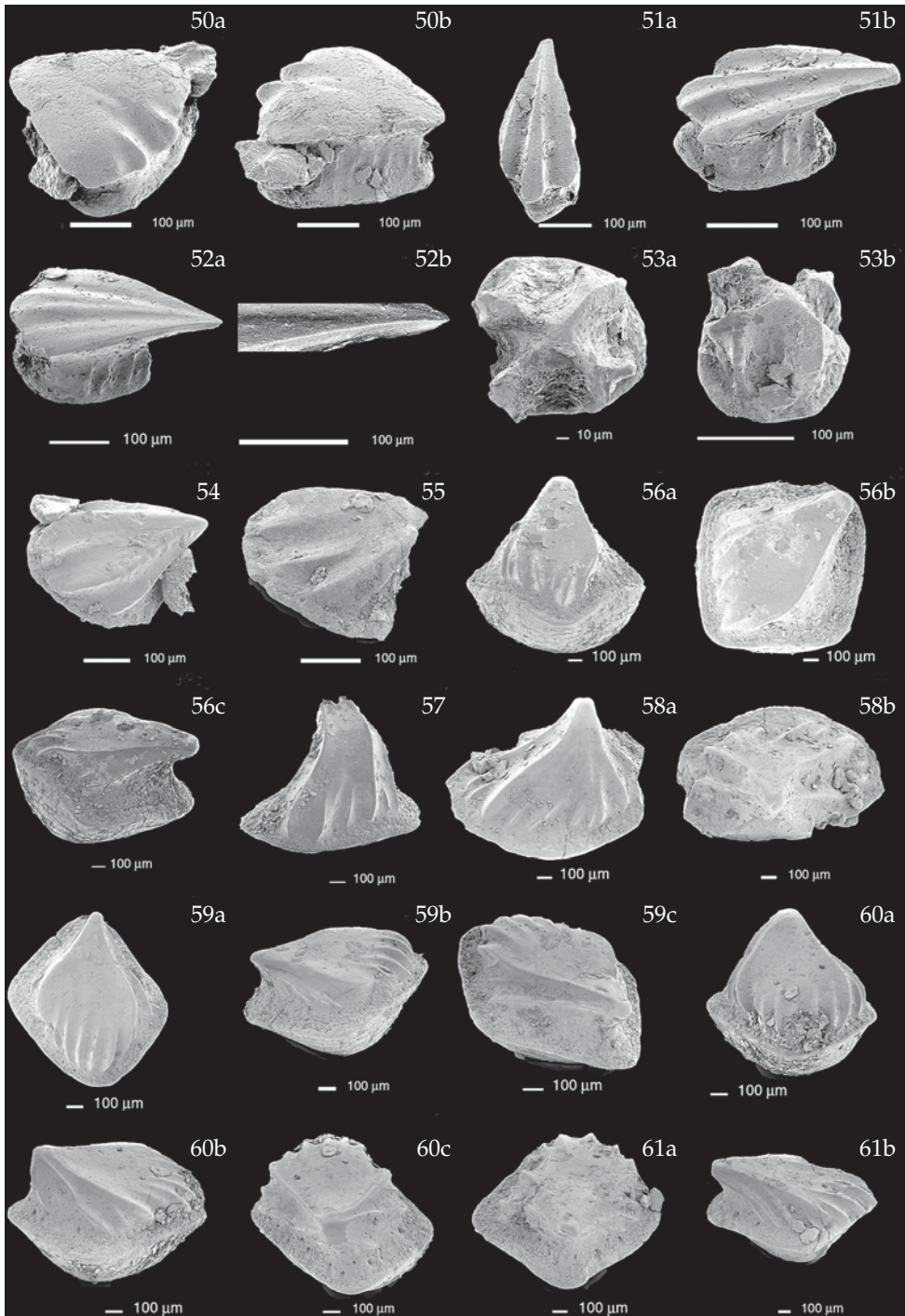


Plate 6 (Figs 62-71b)

Figs 62-71b. Scleritome of *Nostolepis striata*. *Nostolepis striata* Pander, 1856 *sensu* Gross 1947, 1971.
Figs 62-67. 'Modified' trunk scales.

- Fig. 62. P9190. (a) Anterior view. (b) Posterior view.
Fig. 63. P9191. (a) Anterior view. (b) Posterior view.
Fig. 64. P9192. (a) Anterior view. (b) Lateral view. (c) Posterior view.
Fig. 65. P9193. (a) Anterior view. (b) Lateroposterior view.
Fig. 66. P9194. (a) Posterior view. (b) Lateral view. (c) Anterolateral view.
Fig. 67. P9195. (a) Anterior view. (b) Lateral view. (c) Posterior view.
Fig. 68. P9196. Scale from the shoulder girdle (pinnal 'plate')? Ørvig sample. (a) Crown view. (b) Lateral view.
Fig. 69. P9197. Multicrowned scale. (a, b) Anterior views.

Figs 70-71b. Squamae proniae.

- Fig. 70. P9198. (a, b) Orientation unclear. (c) Detail of b.
Fig. 71. P9199. (a) Posterolateral view. (b) Anterior view.

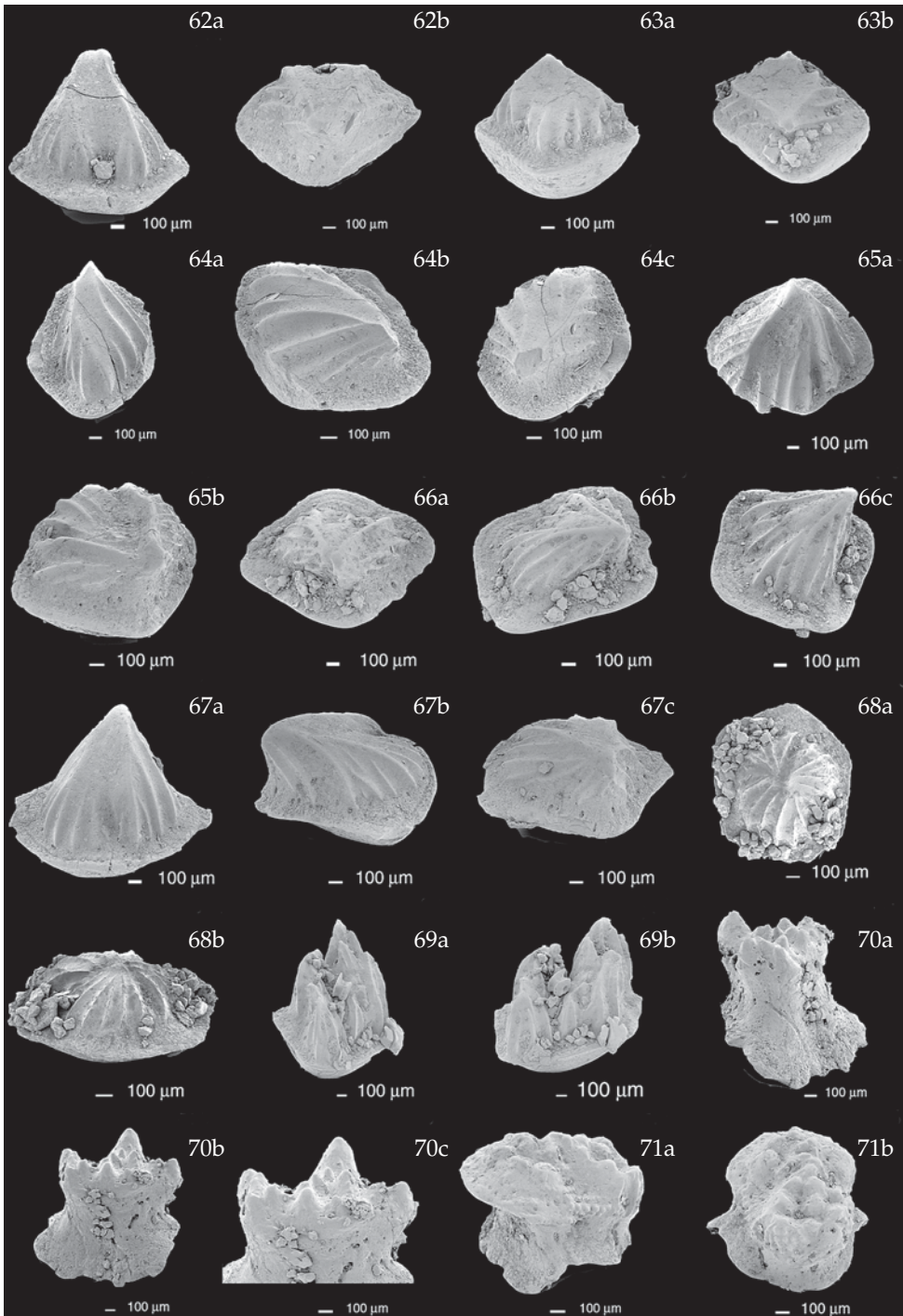


Plate 7 (Figs 71c-81a)

Figs 71c-80. Scleritome of *Nostolepis striata*. *Nostolepis striata* Pander, 1856 *sensu* Gross 1947, 1971.

Fig. 71. P9199. (c) Squama pronia. Detail of Fig. 71b.

Fig. 72. P9200. Arched tooth plate. (a) Posterior view. (b) Lateral view. (c) Anterior view.

Figs 73-80. Spines.

Fig. 73. P9201. (a) Distal view. (b) Anterior view.

Fig. 74. P9202. (a) Lateral view of proximal/anterior end of spine part. (b) Transverse section in more distal part of spine.

Fig. 75. P9203. (a) Proximal/anterior end of spine, seen from above. (b) Transverse section in more distal part of spine.

Fig. 76. P9204. (a) Transverse section in more distal part of spine. (b) Proximal/anterior end of spine, seen from above.

Fig. 77. P9205. (a) Proximal/anterior end of spine, seen from above. (b) View from posterolateral.

Fig. 78. P9206. (a) Leading edge at distal spine end. (b) Detail of lateral ornament near proximal breaking point. (c) Trailing edge in distal view. (d) Detail of trailing edge and distal transverse section.

Fig. 79. P9207. (a) Lateral view at distal end of spine. (b) Detail of ornament near trailing edge. (c) Spine cavity, from proximal.

Fig. 80. P9208. (a) Lateral view at distal end of spine. (b) Ornament near trailing edge.

Fig. 81. P9209, ischnacanthid spine. (a) Leading edge (proximal/anterior to the right).

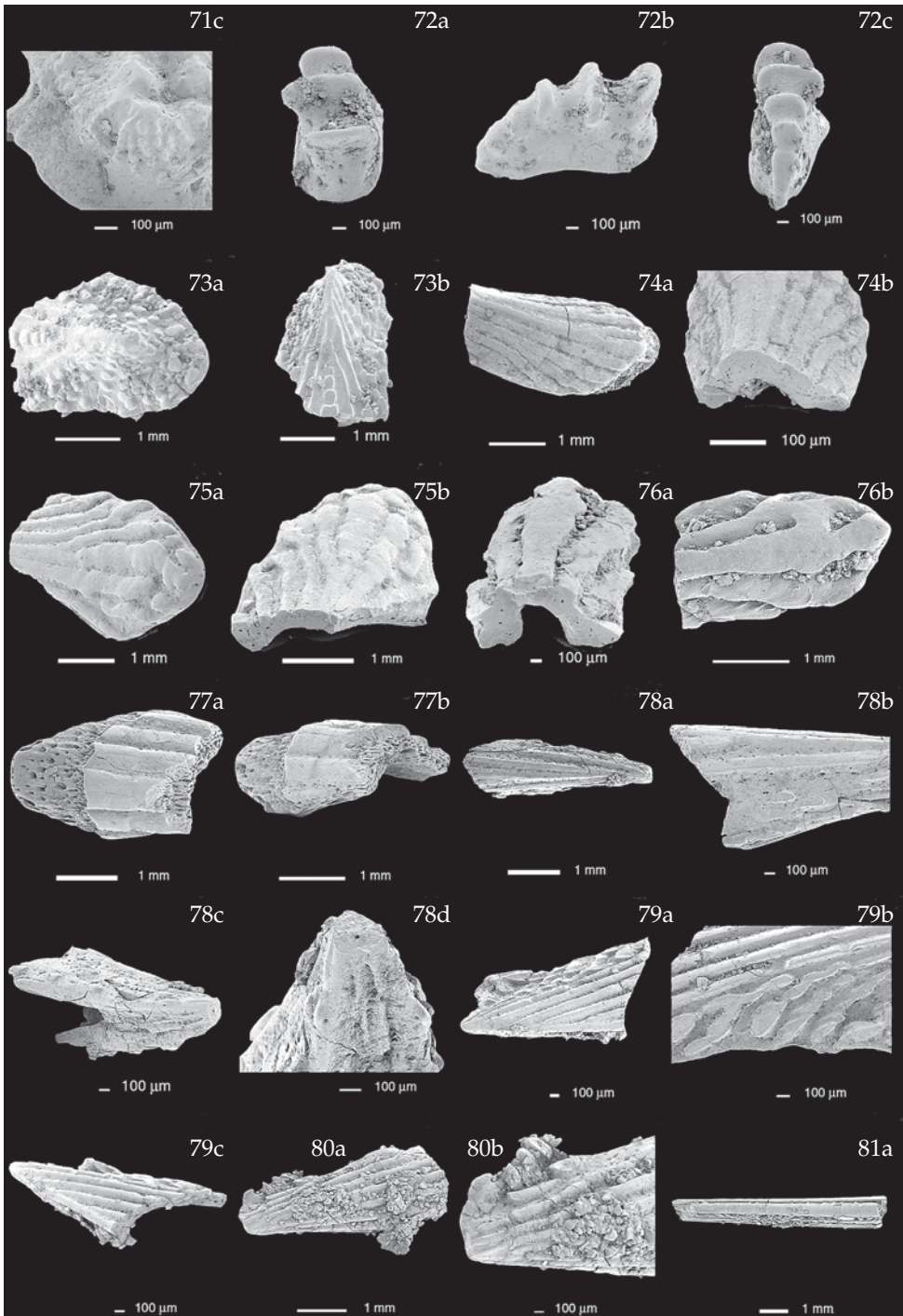


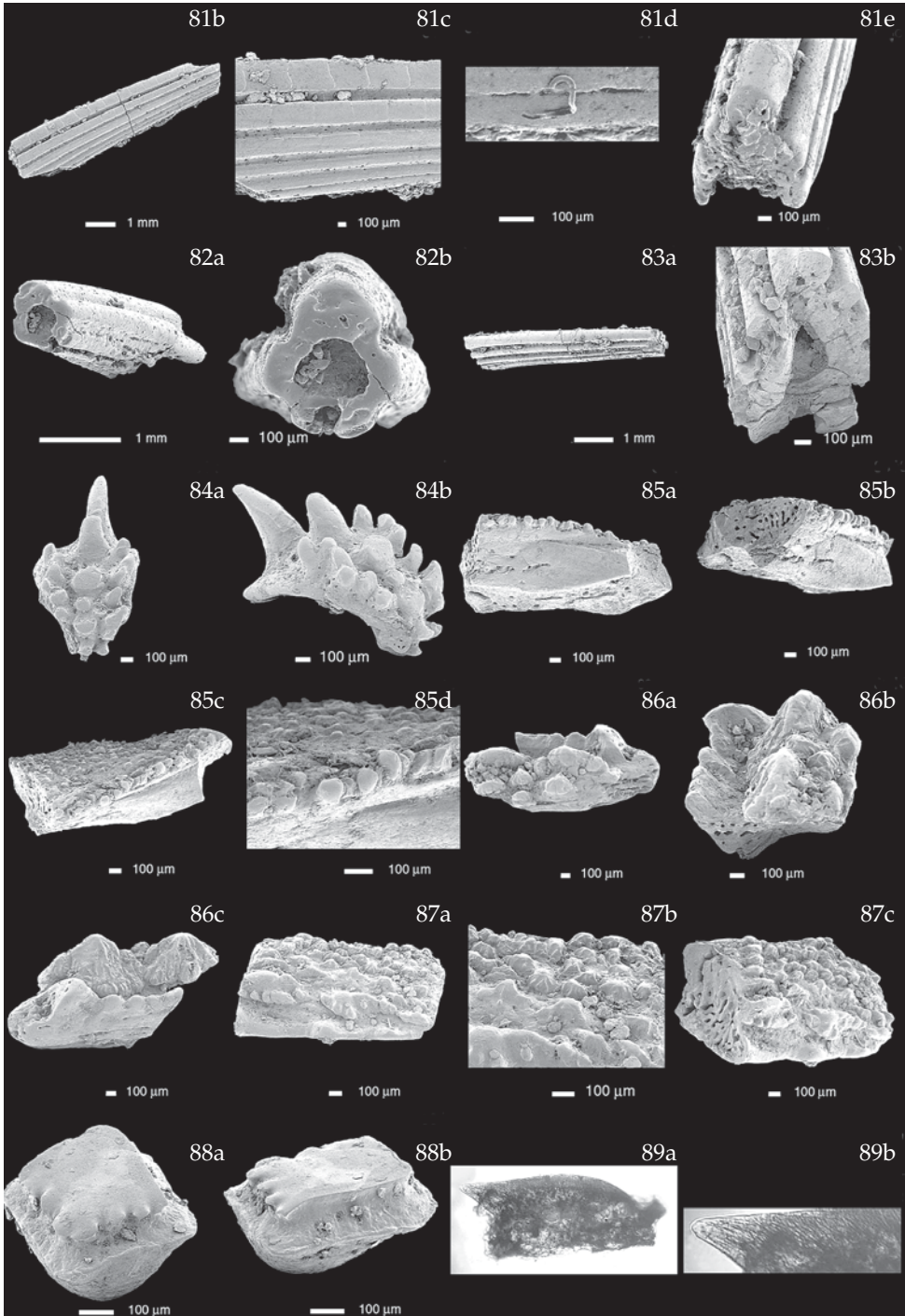
Plate 8 (Figs 81b-89)

Figs 81b-83. Ischnacanthid spines and (Fig. 84) arched tooth plate.

- Fig. 81. P9209. (b) Anterolateral view. (c) Detail of 'Spanish tile' rib ornament. (d) Detail (trace of micro-organism (parasitic worm? Turner, pers. comm.). (e) Transverse section at proximal breaking point.
- Fig. 82. P9210. (a) View from posterolateral, with trailing edge. (b) Transverse section at distal breaking point.
- Fig. 83. P9211. (a) Leading edge, from above and aside. (b) Transverse section at proximal breaking point.
- Fig. 84. P9212. (a) Anterior and occlusal view. (b) Anterolateral view.

Figs 85-87. *Nostolepis striata* scleritome or poracanthodid jawbone fragments.

- Fig. 85. P9213. (a) Occlusal view. (b) Transverse section. (c) Ornament on medial/lingual side. (d) Detail of longitudinal row of tiny blade-like teeth on the medial margin of the biting edge.
- Fig. 86. P9214. (a) Medial/lingual side. (b) Longitudinal view, with transverse section. (c) Labial view.
- Fig. 87. P9215. (a) Medial/lingual side, posteriad/pharyngead to the right. (b) Detail of ornament in a. (c) More occlusal view, with transverse section.
- Fig. 88. P9216, *Gomphonchus volborthi* (Rohon, 1893). (a) Anterior view. (b) Lateral view.
- Fig. 89. P9217. (a) Osteostracan fragment with ridge, c. 100x. (b) Detail of ridge (posterior end to the left). Magnification twice a. Ramsåsa. Sample Q607. For remarks on histology see text.



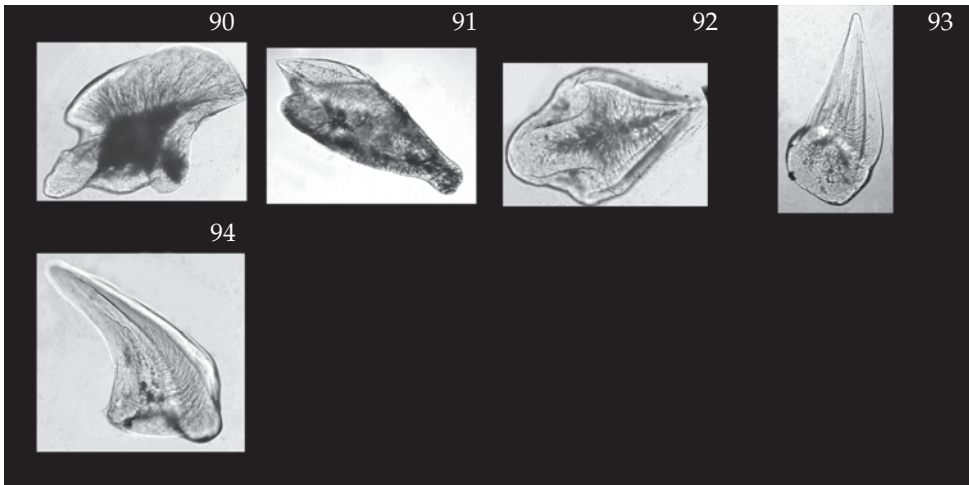


Plate 9 (Figs 90-94)

Magnification c. 400x. For remarks on histology see text. Specimens from Helvetesgraven derive from the residue described by Vergoossen (1999b).

Fig. 90. P9218. *Thelodus* sp. indet., calcarate glabrous scale. *Thelodus parvidens* s.s. or *T. sculptilis* scleritome or other taxon? Helvetesgraven.

Fig. 91. P9219. Forma *Thelodus trilobatus*. Monocuspid scale. Helvetesgraven.

Fig. 92. P9220. *Katoporodus tricavus* (Gross, 1967). Helvetesgraven.

Figs 93-94 *Thelodus* sp. indet., forma *subulata*, new form. Varbla 502 core, depth 19.10 m. Upper Ludlow. Tahula Beds. Lowermost *T. sculptilis* zone. Estonia.

Fig. 93. RGM 323080. Posterior view.

Fig. 94. RGM 323081. Anterior crown view.